

LA-UR-

*Approved for public release;
distribution is unlimited.*

Title:

Author(s):

Submitted to:



Los Alamos National Laboratory, an affirmative action/equal opportunity employer, is operated by the University of California for the U.S. Department of Energy under contract W-7405-ENG-36. By acceptance of this article, the publisher recognizes that the U.S. Government retains a nonexclusive, royalty-free license to publish or reproduce the published form of this contribution, or to allow others to do so, for U.S. Government purposes. Los Alamos National Laboratory requests that the publisher identify this article as work performed under the auspices of the U.S. Department of Energy. Los Alamos National Laboratory strongly supports academic freedom and a researcher's right to publish; as an institution, however, the Laboratory does not endorse the viewpoint of a publication or guarantee its technical correctness.

Form 836 (8/00)

**LA-UR-98-0418, LANL, Los Alamos (1998);
submitted to *Nuclear Science and Engineering***

**Cascade-Exciton Model Analysis of
Nucleon-Induced
Fission Cross Sections of Lead and Bismuth
at Energies from 45 to 500 MeV**

A. V. Prokofiev

V. G. Khlopin Radium Institute, 2nd Murinsky av. 28, St. Petersburg 194021, Russia

and

S. G. Mashnik and A. J. Sierk

T-2, Theoretical Division, Los Alamos National Laboratory, Los Alamos, NM 87545

Abstract—*An extended version of the Cascade-Exciton Model (CEM) of nuclear reactions is applied to analyze nucleon-induced fission cross sections for ^{209}Bi and ^{208}Pb nuclei in the 45–500 MeV energy range. The available data on linear momentum transfer are analyzed as well. The results are compared with analytical approximations resulting from a comparative critical analysis of all available experimental data. Systematic discrepancies between calculations and experimental data are revealed. A modification of the CEM is proposed, which significantly improves the model predictions for projectile energies above 100 MeV.*

I. INTRODUCTION

A large amount of nuclear reaction data, including fission cross sections at intermediate energies is required for applications, e.g., for accelerator transmutation of waste (ATW) for elimination of long-lived radioactive wastes with a spallation source, accelerator-based conversion (ABC) aimed to complete the destruction of weapon plutonium, accelerator-driven energy production (ADEP) which proposes to derive fission energy from thorium with concurrent destruction of the long-lived waste and without the production of weapon-usable material, for accelerator production of tritium (APT) etc. (see the Proceedings of the international conferences on Accelerator-Driven Transmutation Technology held in Kalmar [1] and Dubna [2] and references therein). Experiments to measure these data are costly and there are a limited number of facilities available to make such measurements. Therefore reliable models are required to provide the necessary data.

During the last two decades, several versions of the Cascade-Exciton Model (CEM) [3] of nuclear reactions have been developed at JINR, Dubna (for an overview, see [4]). A large variety of experimental data for reactions induced by nucleons [5], pions [6], and photons [7] has been analyzed in the framework of the CEM and the general validity of this approach has been confirmed. The recent *International Code Comparison for Intermediate Energy Nuclear Data* [8] has shown that the CEM adequately describes nuclear reactions at intermediate energies and has one of the best predictive powers for double differential cross sections of secondary nucleons as compared to other available models (see Tabs. 5 and 6 in the Report [8] and Fig. 7 in Ref. [9]). In the last few years, the CEM has been extended [10] to calculate hadron-induced spallation and used to study [11]–[15] about 700 reactions induced by protons from 10 MeV to 5 GeV on nuclei from Carbon to Uranium.

A detailed description of the CEM may be found in Ref. [3] and of its extended version, as realized in the code CEM95, in Refs. [10, 11]; therefore, we mention here only its basic assumptions. The CEM assumes that reactions occur in three stages. The first stage is the intranuclear cascade in which primary and secondary particles can be rescattered several times prior to absorption by, or escape from the nucleus. The cascade stage of the interaction is described by the standard version of the Dubna intranuclear cascade model (ICM) [16]. The excited residual nucleus remaining after the emission of the cascade particles determines the particle-hole configuration that is the starting point for the second, preequilibrium stage of the reaction. The subsequent relaxation of the nuclear excitation is treated by an extension of the Modified Exciton model (MEM) [17] of preequilibrium decay which also includes the description of the equilibrium evaporative third stage of the reaction.

Recently, the CEM has been extended by taking into account the competition between particle emission and fission at the compound nucleus stage [18] and a more realistic calculation of nuclear level density [19]. An earlier extended version of the CEM, as realized in the code CEM92, was used by Konshin [15] to calculate nucleon-induced fission cross sections for actinides in the energy region from 100 MeV to 1 GeV. Nevertheless, previously the CEM has not been applied to study fission cross sections for pre-actinides; therefore, its predictive power and applicability to evaluate arbitrary fission cross sections was unknown.

In order to investigate the applicability of the CEM to fission cross sections and hoping to learn more about intermediate-energy fission and to identify possible improvements to the CEM and other models to improve their predictive power, we use here an extended version of the CEM (see the recent report [11] and references therein), as realized in the code CEM95 [20], to perform a detailed analysis of proton- and neutron-induced fission cross sections of ^{209}Bi and ^{208}Pb nuclei and of the linear momentum transfer to the fissioning nuclei in the 45–500 MeV energy range.

The ^{208}Pb and ^{209}Bi target nuclei and this energy interval were chosen for this study for the following reasons:

- new experimental information on $^{208}\text{Pb}(n,f)$ and $^{209}\text{Bi}(n,f)$ reactions has been recently obtained at these incident energies (see [21]-[24] and references therein),
- the reactions under study have practical importance in connection with concepts of accelerator-driven transmutation and tritium production technologies, which may include the use as a neutron source of massive lead or lead-bismuth targets irradiated by proton beams,
- cross sections for these reactions are widely used as standards in the intermediate energy region (e.g., [25, 26]), with cross sections for other targets being normalized to them,
- fissioning nuclei in this mass region are close to the doubly magic nucleus ^{208}Pb , where one would expect the clearest manifestation of shell effects, which are important for the development of any model,
- fission barriers of nuclei in this mass region do not have the double-humped structure which appears in the actinide nuclei and makes calculations for them more complicated and uncertain.

II. CALCULATIONAL TECHNIQUE

As the fission cross sections for nuclei under study constitute a small part of the total reaction cross section, the statistical weight method [18, 27] is used to calculate fission cross sections instead of the straightforward Monte-Carlo technique. It allows us to obtain statistical uncertainties of the calculated fission cross sections, as a rule, not more than 5–10% with only 3000 inelastic events in each calculation.

In the course of the calculations, the characteristics of the fissioning nuclei (the charge, the mass, the excitation energy, all components of the linear and angular momenta, and the statistical weight of the event) are saved, and later used for the construction of distributions of fission events with respect to specified parameters as well as for the calculation of the corresponding average values. Examples of these distributions are shown in Figs. 1 and 2.

Fig. 1 represents the distributions of calculated longitudinal linear momentum transfer (LMT) to the fissioning nuclei in the $^{209}\text{Bi}(p,f)$ reaction for incident proton energies of 45 MeV (a), 73 MeV (b), 96 MeV (c), and 160 MeV (d). Comparing these distributions allows one to follow the changes in the reaction mechanism with increasing incident particle

energy. The calculation predicts that most nuclei undergoing fission induced by 45 MeV protons possess a linear momentum equal to that of the incident proton (Fig. 1a), i.e., the full LMT mode predominates, which corresponds to fission from the compound nucleus. (Hereinafter the term “compound nucleus” implies the nucleus with the charge and the mass equal to the sum of the corresponding characteristics of the target nucleus and of the incident particle.) With increasing incident proton energy, the share of the events with the full LMT falls quickly (Fig. 1b). For proton energies of 100 MeV or more (Fig. 1c, d) the fission from the compound nucleus practically “dies out”; the maximum in the distribution becomes displaced to the region of incomplete LMT and the distribution width increases. A comparison of the LMT calculations with experimental data is discussed in Sect. III.

Fig. 2 shows the distributions of the charge of the fissioning nuclei (a, b), mass (c, d), and excitation energy (e, f) in the $^{209}\text{Bi}(p,f)$ reaction for proton energies of 45 and 160 MeV. The curves reflect the same tendency as discussed above. At 45 MeV, fission from the compound nucleus (^{210}Po) predominates. On the contrary, at 160 MeV the distributions become displaced and their shape approaches symmetry.

In Fig. 3, we show the dependence of the average charge (a), mass (b) and excitation energy (c) of the fissioning nuclei in the $^{209}\text{Bi}(p,f)$ and $^{209}\text{Bi}(n,f)$ reactions as functions of the incident particle energy in the 45–160 MeV range. The energy dependence of the average mass and excitation energy of the fissioning nuclei are nearly the same for these two reactions. On the other hand, the average charge of the fissioning nuclei for the (p,f) reaction decreases faster than for the (n,f) one. This can be qualitatively explained by noticing that there is a significant probability that the incident nucleon leaves the nucleus after an inelastic scattering during the intranuclear cascade stage of the reaction.

The results presented in this and subsequent sections are obtained with input parameters of CEM95 as discussed in Sect. V.

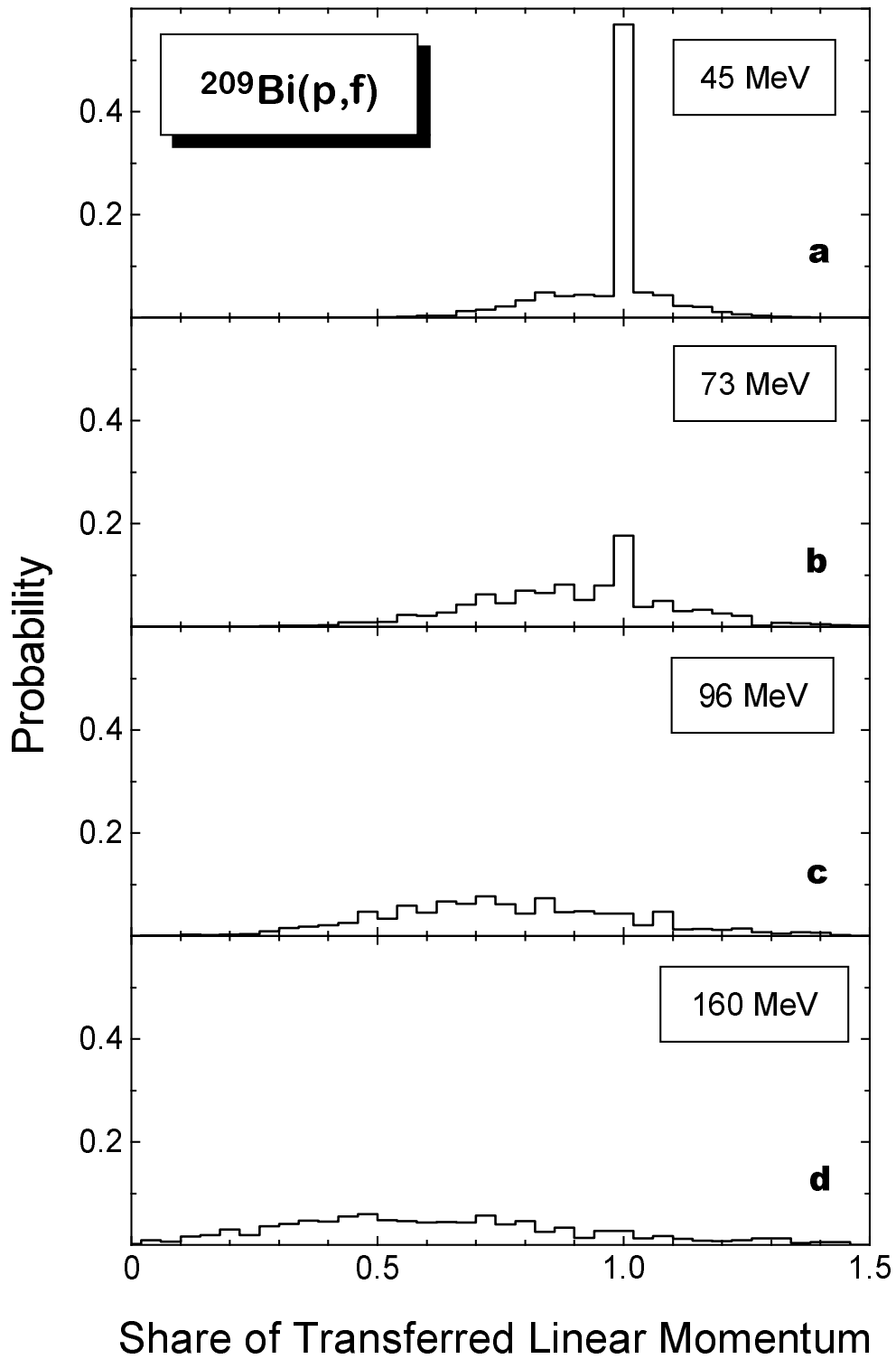


Fig. 1. Calculated distributions of longitudinal linear momentum transferred to the fissioning nuclei in the $^{209}\text{Bi}(p,f)$ reaction for incident proton energies of 45 MeV (a), 73 MeV (b), 96 MeV (c), and 160 MeV (d).

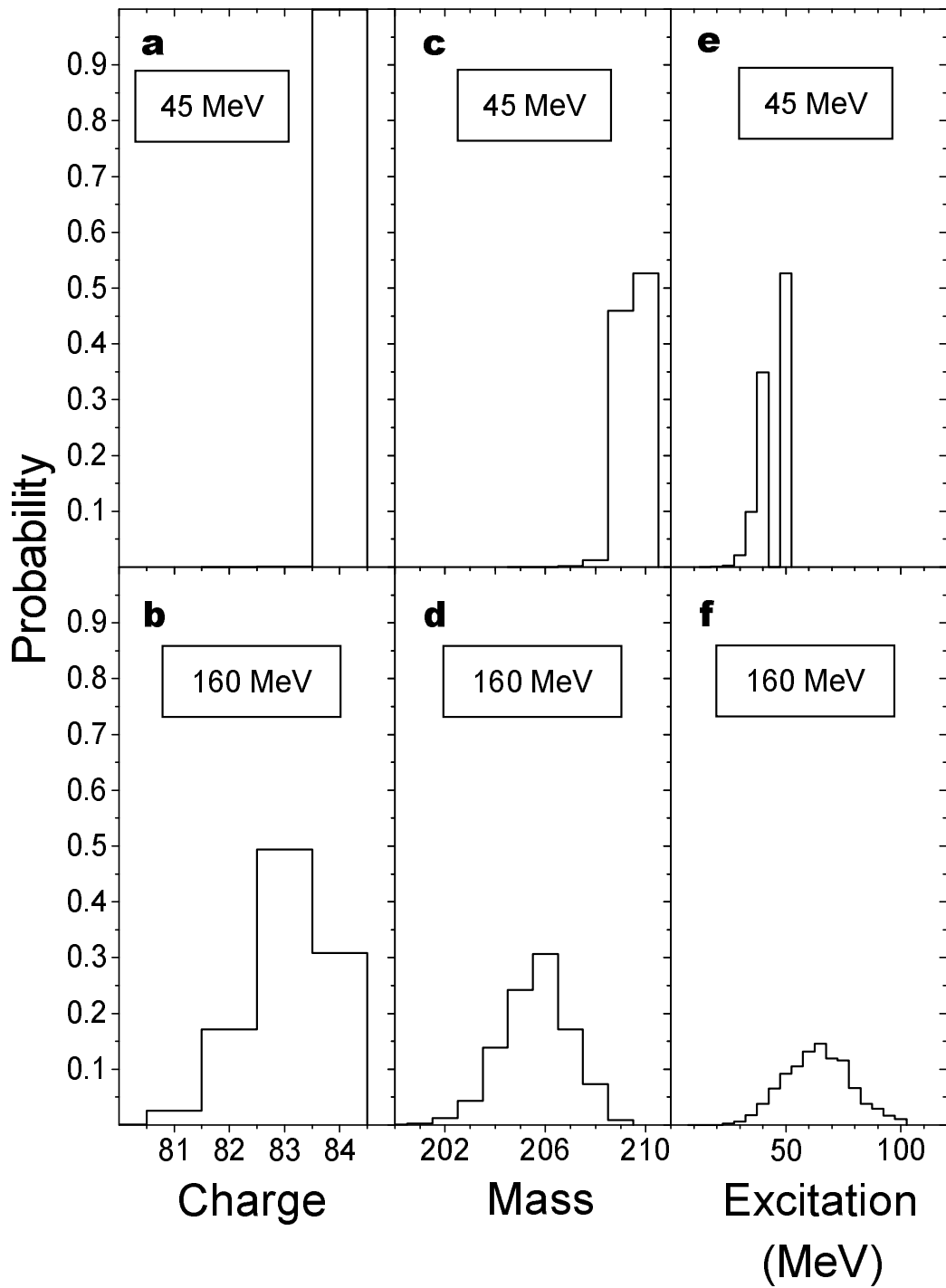


Fig. 2. Calculated distributions of fissioning nuclei in the $^{209}\text{Bi}(p,f)$ reaction vs. charge (a,b), mass (c,d), and excitation energy (e,f) for incident proton energies of 45 MeV (a,c,e) and 160 MeV (b,d,f).

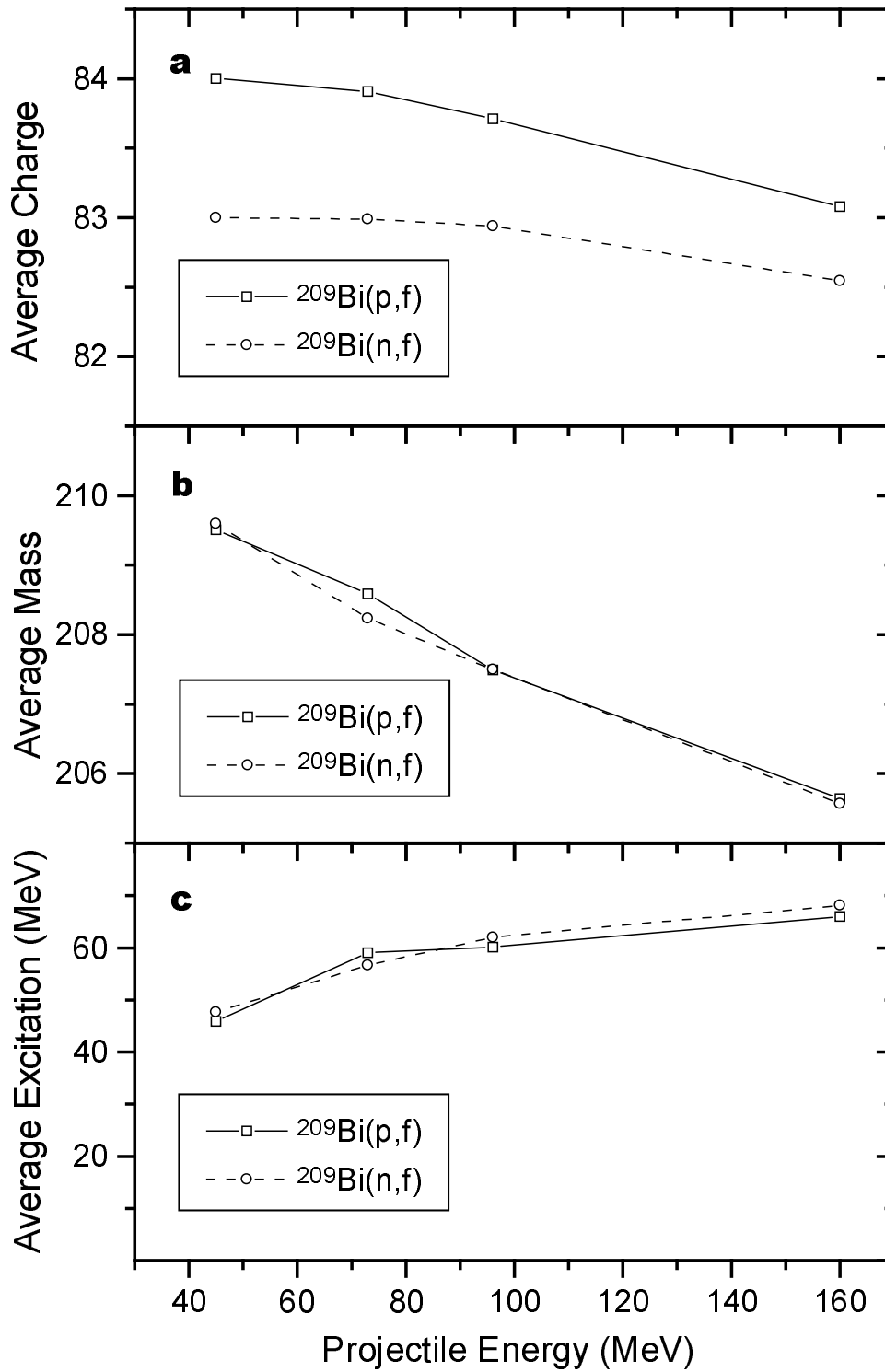


Fig. 3. Calculated average charge (a), mass (b), and excitation energy (c) of fissioning nuclei in the $^{209}\text{Bi}(p,f)$ reaction as a function of projectile energy.

III. LINEAR MOMENTUM TRANSFER

It has been previously shown that the momentum transferred in nucleon reactions with actinide nuclei is better described by the CEM than by other models (see details in Ref. [28]).

Fig. 4 shows the calculated average LMT for the $^{209}\text{Bi}(p,f)$ (a), $^{209}\text{Bi}(n,f)$ (b), $^{208}\text{Pb}(p,f)$ (c), and $^{208}\text{Pb}(n,f)$ (d) reactions in comparison with the sparse available experimental data [29]–[32]. A large spread exists between the $^{209}\text{Bi}(p,f)$ LMT data from different authors (Kowalski [29], Stephan [30], Shigaev [31]) and even within the same experimental dataset [31]. This may indicate the presence of some omitted systematic uncertainties in that work [31], which was performed with solid-state nuclear track detectors. Possible sources of systematic uncertainty may include a decrease of detection efficiency at back angles, fluctuations of the position of the beam at the target, as well as inhomogeneity of the target. We regard as more reliable the data from the works [29, 30] where fission fragments were registered by semiconductor detectors in coincidence mode. Judging from these data, one can conclude that our present CEM95 calculation predicts correctly a decrease with energy of the average LMT for the $^{209}\text{Bi}(p,f)$ reaction but underestimates its average value by 1–1.5 times the experimental uncertainty for the highest energy.

To the best of our knowledge, only one experimental work is available on LMT for the (n,f) type of reactions [32] (see Fig. 4b). In this work the average LMT was obtained for the $^{209}\text{Bi}(n,f)$ reaction at 75 MeV by measuring the difference between the kinetic energies of the fission fragments registered by an ionization chamber in the forward and backward hemispheres. In contrast to the $^{209}\text{Bi}(p,f)$ results, the average LMT calculated with the CEM95 code lies above the sole experimental point by about 1.5 times the experimental uncertainty.

The works of Kowalski [29] and Stephan [30] also include measurements of LMT distributions for the fissioning nuclei in the $^{209}\text{Bi}(p,f)$ reaction at 156 and 96 MeV, respectively. To a first approximation, the distributions are Gaussian-shaped, similar to the CEM95 predictions (see Fig. 1c, d). For a quantitative comparison between the calculations and experiment, we calculate the second moment (dispersion) of the LMT experimental and calculated distributions. In order to compare the experimental dispersion with the calculated one, it is necessary to introduce a correction to the latter, which takes into account the prompt neutron emission from the fission fragments. We estimate this correction using the average kinetic energy of the prompt fission neutrons from Ref. [33] and the average number of neutrons per fission from Ref. [34]. The comparison between calculated and experimental results is shown in Table I.

Table I shows that there is good agreement between the experimental data and our results corrected for the prompt neutron emission from the fission fragments.

On the whole, we conclude that the description of linear momentum transfer processes provided by CEM95 does not contradict the available experimental data.

In Sect. VI we discuss a sensitivity study of the calculated fission cross sections to different input parameters of CEM95. We also study the sensitivity of the LMT description. It is found that neither the average nor the dispersion of the LMT varies beyond the statistical uncertainties of the calculations for any reasonable variation of the input parameters.

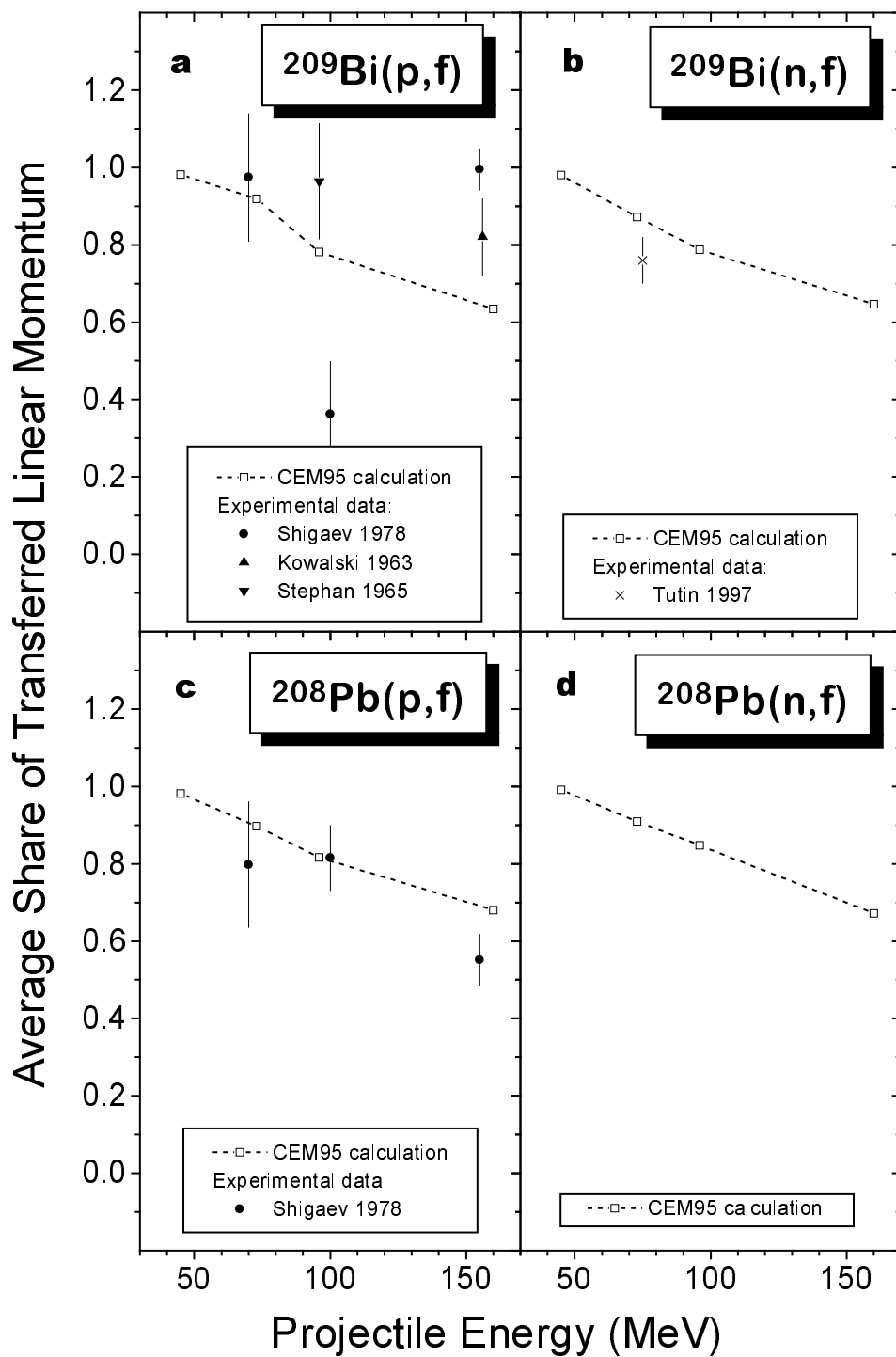


Fig. 4. The average share of the linear momentum transferred to the fissioning nuclei as a function of the projectile energy, for the following reactions: $^{209}\text{Bi}(p,f)$ (a), $^{209}\text{Bi}(n,f)$ (b), $^{208}\text{Pb}(p,f)$ (c), and $^{208}\text{Pb}(n,f)$ (d). The points are experimental data from Refs. [29]–[32]. The dashed lines and the open squares represent the present calculations.

This insensitivity can be interpreted as follows. The momentum losses occur mainly at the cascade stage of the reaction due to forward-peaked emission of fast cascade particles. As the excited nucleus nears statistical equilibrium, the secondary particles become less energetic and their emission becomes more isotropic in the center-of-mass system. Thus the secondaries being emitted at the later reaction stages take away less and less momentum. Since the free parameters available in CEM95 relate only to these later reaction stages, it is natural that their variations have only a weak influence on the resulting LMT distributions.

TABLE I
Dispersion of the LMT distribution in the $^{209}\text{Bi}(p,f)$ reaction
(in units of the incident proton linear momentum)

Proton energy (MeV)	CEM95 results (uncorrected)	Correction due to prompt neutron emission by fission fragments	CEM95 corrected results	Experimental data
96	0.25	0.28	0.38	0.36 ± 0.02 [30]
160	0.32	0.21	0.38	$0.38 \pm 0.02^*$ [29]

* The experimental value was obtained at the proton energy of 156 MeV.

Furthermore, no notable differences are seen between the calculated LMT data for incident protons and neutrons of the same energy. The calculated results for ^{208}Pb and ^{209}Bi target nuclei are also similar. Thus, CEM95 predicts a weak sensitivity of the LMT processes to variations of the incident particle charge as well as to the target nucleus charge and mass.

IV. APPROXIMATING EXPERIMENTAL FISSION CROSS SECTIONS

In contrast to the poor experimental database for LMT, the measurements of fission cross sections for ^{208}Pb and ^{209}Bi are numerous although their reliability varies greatly. Thus the most effective way to estimate the quality of the model predictions is a comparison of the calculated results with approximations built on the basis of the experimental data taking into account differences in their systematic and statistical uncertainties.

Prokofiev and co-authors [35] performed a literature search and a comparative critical analysis, ranking the experimental data on the (p,f) cross sections for a wide range of nuclei from Ta to U in the energy region up to 30 GeV. We consider only the data for ^{208}Pb and ^{209}Bi up to 500 MeV. An approximation for the $^{209}\text{Bi}(n,f)$ cross section was suggested by Smirnov and published in Ref. [26]. The approximation given below for the $^{208}\text{Pb}(n,f)$ cross section is obtained here and has not been published previously.

A list of publications containing the experimental data on the nucleon-induced fission cross sections for ^{208}Pb and ^{209}Bi is given in Table II.

TABLE II

References to publications containing experimental data on the nucleon-induced fission cross sections for ^{208}Pb and ^{209}Bi at energies up to 500 MeV

Target nucleus	Incident particle	
	p	n
^{209}Bi	[29, 30], [36]–[50]	[21]–[24], [52, 53]
^{208}Pb	[36, 37, 39, 48, 50]	[51, 53], [21]–[23]

The experimental data from the publications listed in Table II were subjected to a critical comparative analysis [35] in order to establish how reliably the quantities defining fission cross sections (incident particle flux, target thickness, fission fragment detection efficiency, etc.) were measured. As a result of this analysis, “reliability grades” were assigned to every dataset based on the following criteria:

- the 1st (highest) grade was assigned to a dataset if the analysis did not reveal any omitted or underestimated sources of systematic uncertainties. Thus, the uncertainties of the 1st-grade data were taken from the original publications,
- the 2nd (medium) grade was assigned to a dataset if there were some omitted or underestimated sources of systematic uncertainties that could be deduced. Thus, enhanced uncertainties were assigned to the 2nd-grade data,
- the 3rd (lowest) reliability grade was assigned to a dataset if the analysis revealed defects leading to large and unpredictable systematic errors. The 3rd-grade datasets were removed from further consideration. Data remeasured or reprocessed by their author(s) in later publications were also not considered.

The reliability grade of a dataset was lowered if an original publication does not contain a detailed description of the experimental technique.

The highest grade was assigned, as a rule, to the datasets obtained by modern techniques: ionization chambers (for the (n,f) reactions), semiconductor detectors, thin film breakdown counters, solid state nuclear track detectors with good geometrical conditions. On the other hand, the datasets obtained by the nuclear photo-emulsion technique or by fission product yield summation generally received the lowest grade.

In a few cases, two or more datasets show a similar energy dependence of the cross section but different absolute values. In these cases, renormalization based on the most reliable absolute cross sections was performed before fitting.

A few experiments were done with natural Pb targets. In order to compare these data with those for pure ^{208}Pb targets, a search was performed for experiments in which (p,f) cross sections were measured for Pb isotopes [36, 37, 39, 50]. Then auxiliary approximations were determined for the $^{206}\text{Pb}/^{208}\text{Pb}$ and $^{207}\text{Pb}/^{208}\text{Pb}$ proton-induced fission cross section ratios (see Fig. 5a, b). The following expression was suggested:

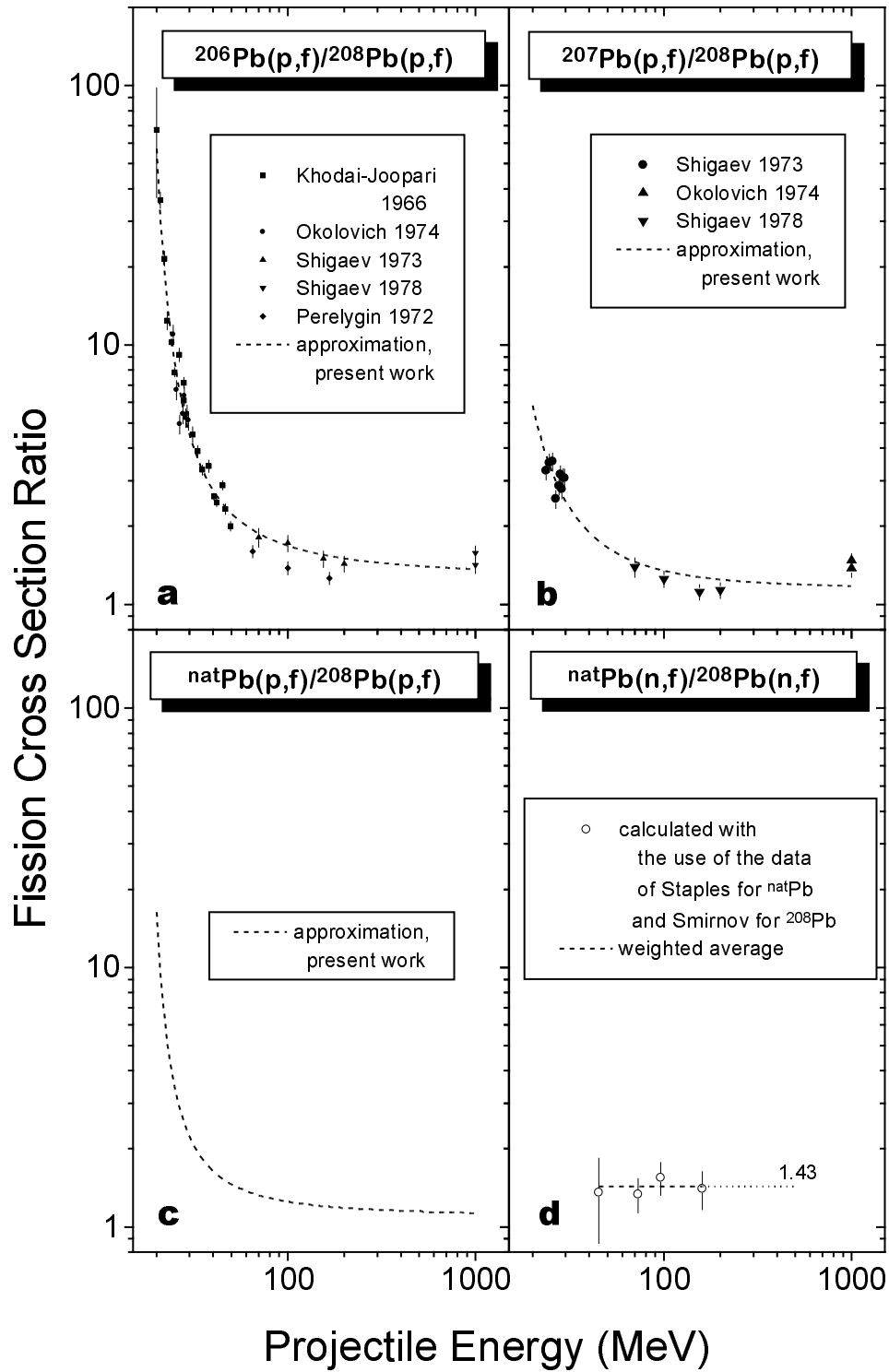


Fig. 5. The experimental data [36, 37, 39, 50] and the approximations of the cross section ratios: $^{206}\text{Pb}(p,f)/^{208}\text{Pb}(p,f)$ (a), $^{207}\text{Pb}(p,f)/^{208}\text{Pb}(p,f)$ (b), $^{\text{nat}}\text{Pb}(p,f)/^{208}\text{Pb}(p,f)$ (c), and $^{\text{nat}}\text{Pb}(n,f)/^{208}\text{Pb}(n,f)$ (d).

$$r(E) = r_0 \exp \frac{b}{(\ln E/E_0)^p}, \quad (1)$$

where $r(E)$ is the cross section ratio, E is the incident particle energy, r_0 , b , E_0 and p are fitting parameters found by the least-square method and given in Table III. χ^2/ν refers to the standard χ^2 per degree of freedom

TABLE III
The parameters of the $^{206}\text{Pb}/^{208}\text{Pb}$ and $^{207}\text{Pb}/^{208}\text{Pb}$ proton-induced fission cross section ratio approximations

Cross section ratio	r_0	b	E_0	p	χ^2/ν
$^{206}\text{Pb}/^{208}\text{Pb}$	1.26	0.975	12.8	1.69	4.89
$^{207}\text{Pb}/^{208}\text{Pb}$	1.15	16.7	3.10	3.74	3.40

Combining these approximations with the natural Pb isotopic composition, we determined an approximation for the $^{nat}\text{Pb}/^{208}\text{Pb}$ (p,f) cross section ratio (see Fig. 5c). This ratio decreases with incident proton energy and becomes nearly constant at an energy of a few hundred MeV.

There are no experiments that include neutron-induced fission cross section measurements for the relevant separated Pb isotopes within the same experiment. Thus the $^{nat}\text{Pb}/^{208}\text{Pb}$ (n,f) cross section ratio was calculated with the use of the ^{nat}Pb data of Staples et al. [21] and the ^{208}Pb data of Smirnov et al. [22, 23] (see Fig. 5d). The ratio is constant within the experimental uncertainties and is equal to 1.43 ± 0.13 in the 45–160 MeV energy region where the data overlap. Assuming that this ratio weakly depends on energy in the 160–500 MeV region, which is true for (p,f) reactions discussed above, a renormalization was performed for the ^{nat}Pb data of Reut [51], Goldanskiy [53], and Staples [21].

Figs. 6–9 show the experimental data on the nucleon-induced fission cross sections for ^{208}Pb and ^{209}Bi together with the corresponding approximations described by the following expressions:

$$\sigma_f(E) = \exp(c_0 + c_1 E + c_2 E^2), \quad (2)$$

$$\sigma_f(E) = \exp[c_0 + c_1 \ln E + c_2 (\ln E)^2], \quad (3)$$

$$\sigma_f(E) = c_0 \{1 - \exp[-c_1(E - c_2)]\}, \quad (4)$$

where σ_f is the fission cross section, E is the incident particle energy, and c_0 , c_1 and c_2 are fitting parameters found by the least-square method and given in Table IV.

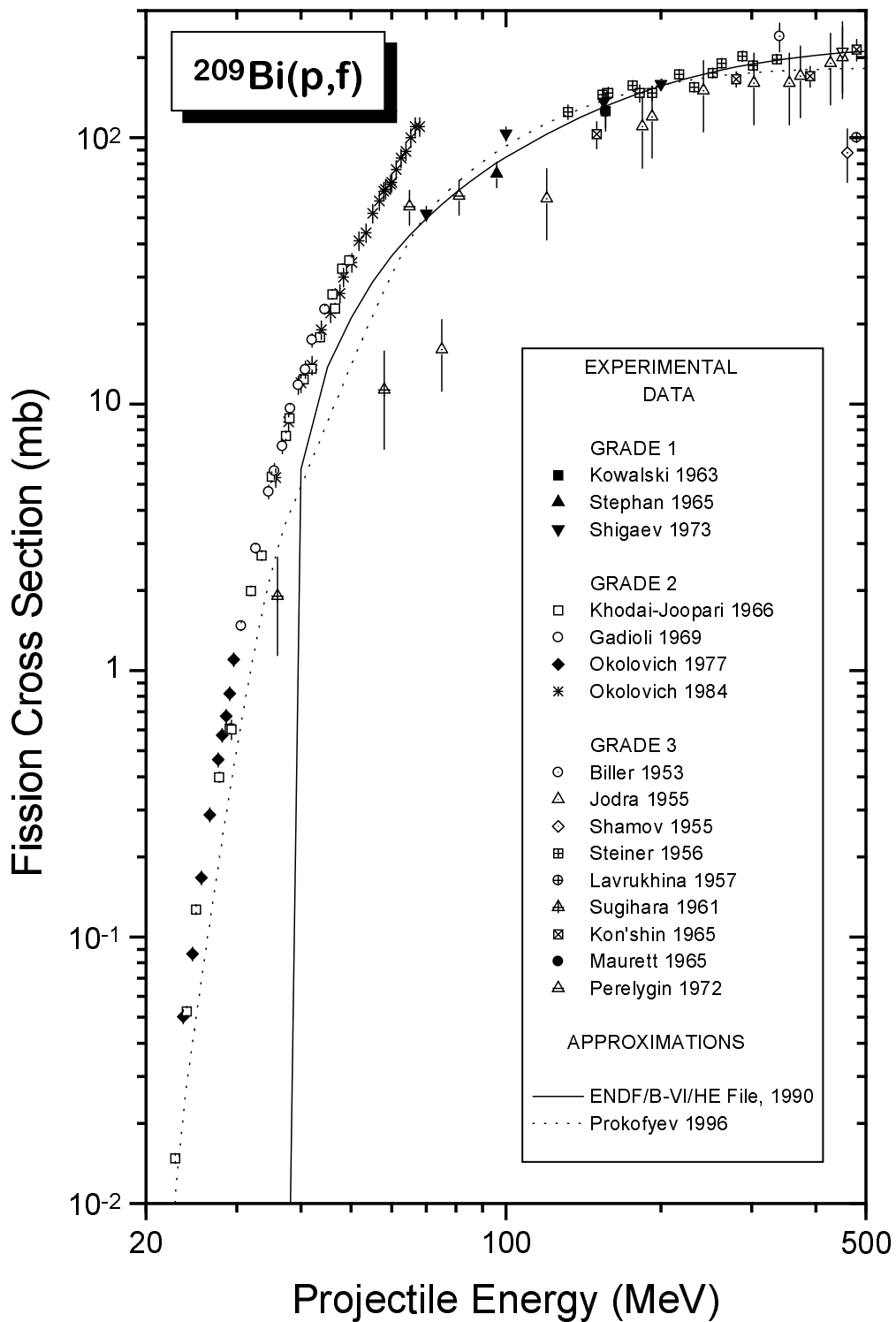


Fig. 6. The experimental data [29]–[31], [37],[39]–[42], [44]–[50] and approximations [35, 54] for the $^{209}\text{Bi}(p,f)$ cross section.

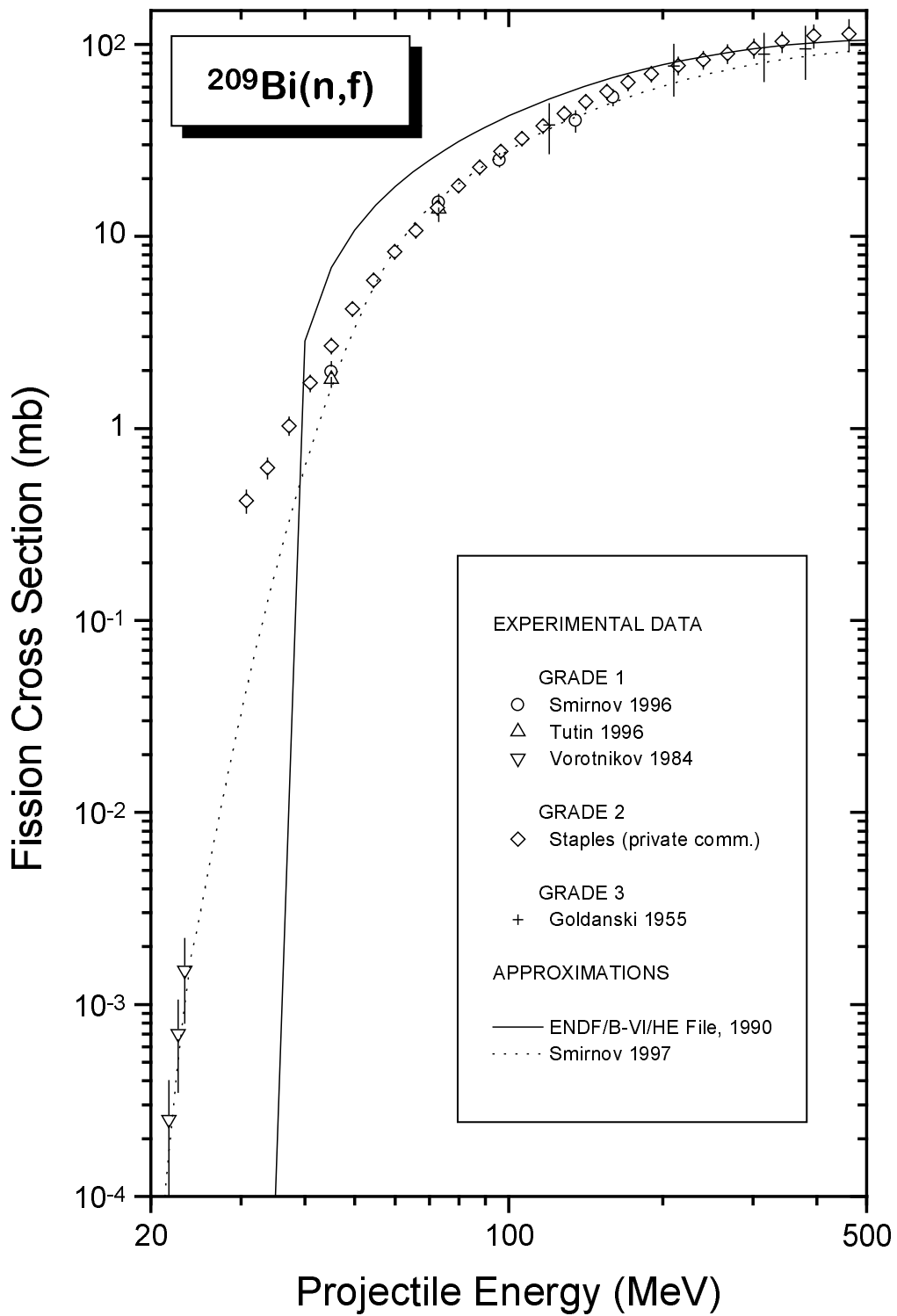


Fig. 7. The experimental data [21, 23, 24, 52, 53] and approximations [26, 54] for the $^{209}\text{Bi}(n,f)$ cross section.

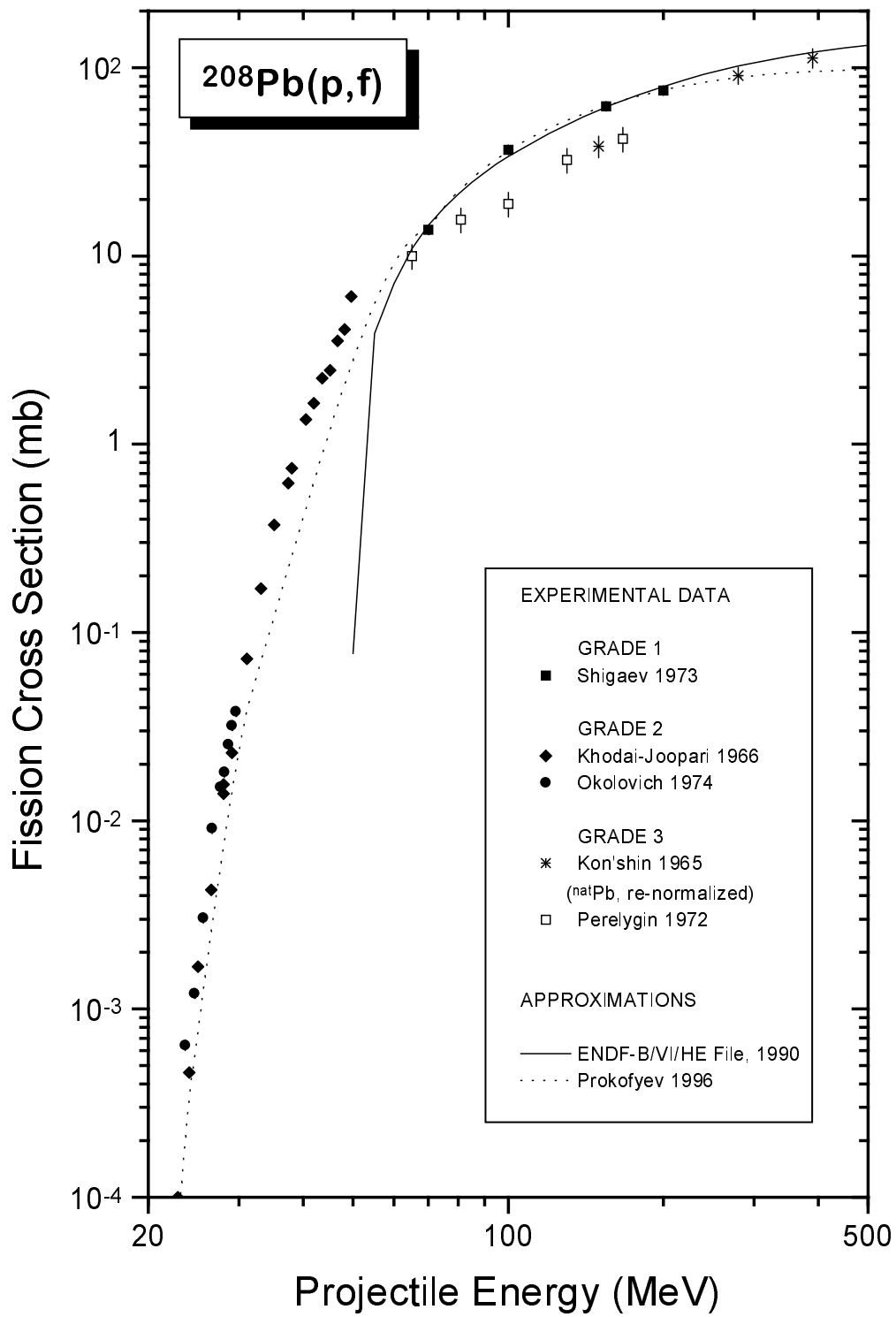


Fig. 8. The experimental data [36, 37, 39, 48, 50] and approximations [35, 54] for the $^{208}\text{Pb}(p,f)$ cross section.

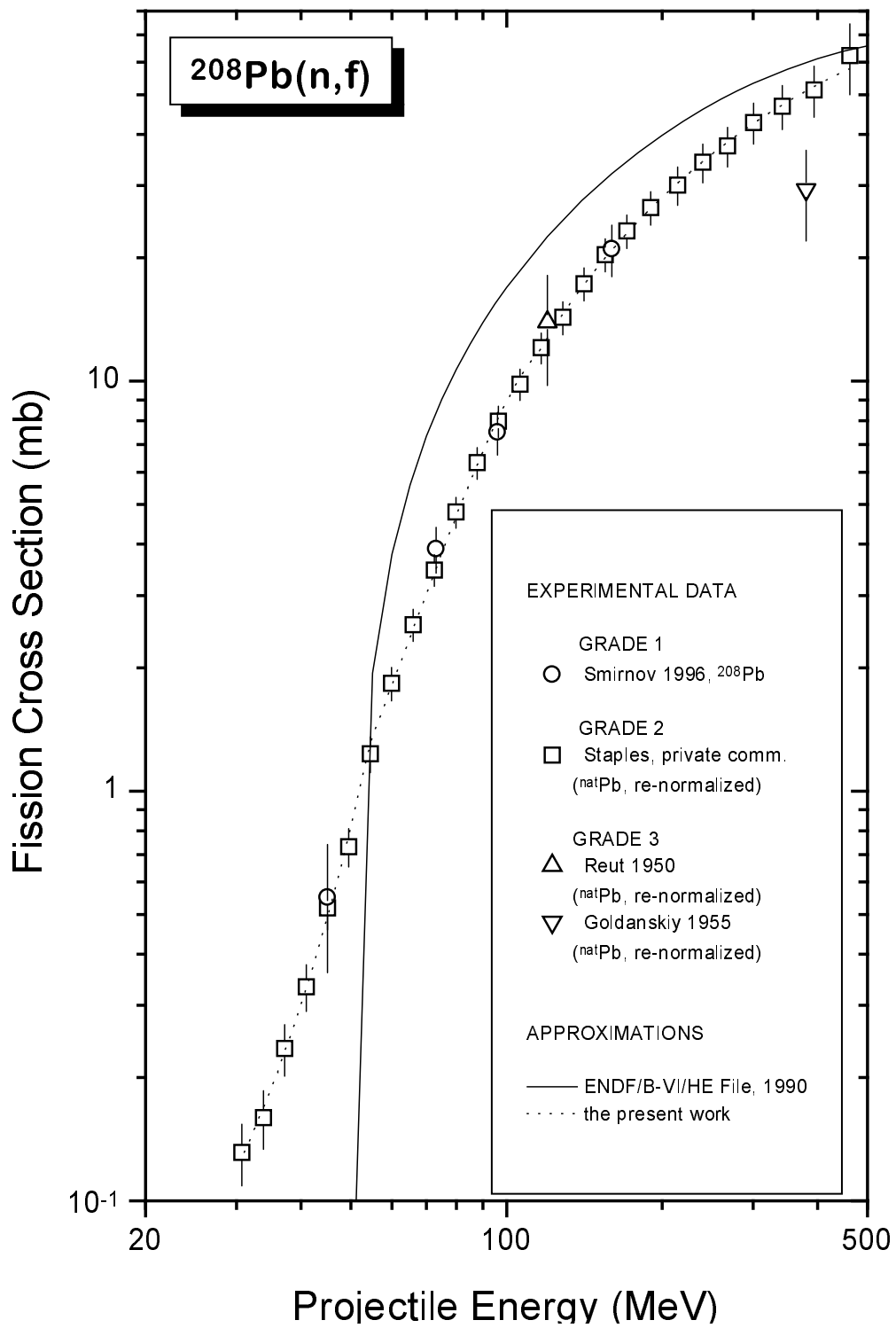


Fig. 9. The experimental data [51, 53], [21]–[23] and approximations [54] for the $^{208}\text{Pb}(n,f)$ cross section.

TABLE IV

The parameters of the nucleon-induced fission cross section approximations for ^{208}Pb and ^{209}Bi

E (MeV)	Expression	c_0	c_1	c_2
$^{209}\text{Bi}(p,f)$				
37.4-70	(2)	-5.150	0.2203	-0.001290
70-3000	(4)	182.7	0.01264	43.60
$^{209}\text{Bi}(n,f)$				
20-73	(3)	-108.7	50	-5.6
73-1000	(4)	100	0.006	45
$^{208}\text{Pb}(p,f)$				
31.1-70	(2)	-16.11	0.5310	-0.003760
70-23000	(4)	98.75	0.01012	55.05
$^{208}\text{Pb}(n,f)$				
30.5–54.5	(2)	-4.455	0.06642	$3.753 \cdot 10^{-4}$
54.5–116.8	(2)	-4.151	0.1026	$-3.920 \cdot 10^{-4}$
116.8–462.4	(4)	80.71	$3.190 \cdot 10^{-3}$	66.06

The approximations of Fukahori and Pearlstein [54] included in the ENDF/B-VI/High Energy files are also shown in Figs. 6–9. They are seriously discrepant with respect to the experimental data below about 40–50 MeV for all four reactions. In the 50–500 MeV region there are discrepancies of up to a factor of 2 between Fukahori’s (n,f) cross section approximations and those given in the present work, which take into account the recent experimental data [21]–[24]. The discrepancy for the (p,f) cross section approximations is less (no more than 35%). We consider the approximations given in the present work as more reliable because they utilize a more complete experimental database and are obtained as the result of the consistent procedure of experimental data ranking and selection.

V. MODELING FISSION CROSS SECTIONS

The nucleon-induced fission cross section calculations for ^{208}Pb and ^{209}Bi nuclei at 45–500 MeV performed in the present work with the code CEM95 show that there is no universal input parameter set that allows us to describe the fission excitation functions in the whole energy region considered. In the lower energy part (up to 160 MeV) the best agreement with the experimental data is reached with the parameter set presented in Tables V and VI. Hereinafter the parameter names are given as in the CEM95 code manual [20].

Fig. 10 illustrates the results of the calculations with the given parameters in comparison with the experimental data approximations discussed in Sect. IV.

The calculations reproduce the general trends of the experimental data, although the model systematically underestimates the cross sections in the middle of the energy range under study (at about 70–100 MeV) and overestimates them at the ends (i.e., above 100–150 MeV as well as below 50–60 MeV). An exception is the $^{208}\text{Pb}(n,f)$ reaction, for which

the calculated results lie under the experimental data for neutron energies below 70 MeV. This discrepancy may be evidence that the data approximation for the $^{208}\text{Pb}(n,f)$ cross section overestimates the actual cross section at low energies, due to an undetermined systematic error in Ref. [21]. This approximation was deduced in Sect. IV by renormalization of the data of Staples [21] assuming that the $^{nat}\text{Pb}(n,f)/^{208}\text{Pb}(n,f)$ cross section ratio does not depend on neutron energy (see Fig. 5d). It is possible that this ratio rises with neutron energy decrease below 50–70 MeV, similarly to the $^{nat}\text{Pb}(p,f)/^{208}\text{Pb}(p,f)$ cross section ratio (see Fig. 5c), but the lack of $^{208}\text{Pb}(n,f)$ cross section data does not allow us to make a quantitative estimate.

TABLE V

Optimal CEM95 input parameters for nucleon-induced fission cross section calculations for ^{208}Pb and ^{209}Bi targets in the 45–160 MeV region

Parameter name and recommended value	Parameter description
RM=1.5	The parameter r_0 (fm) in Dostrovsky's formula [55] for inverse reaction cross sections
WAM (see Table VI)	The ratio of the level density parameters in the fission and neutron emission channels, a_f/a_n
IFAM=9	The choice of level density parameter systematics $a(Z, N, E^*)$: the 3rd Iljinov et al. systematics [56]
IB=6	The choice of macroscopic fission barrier model $B_f(Z, N)$: Krappe, Nix, and Sierk [57]
ISH=2	The choice of shell correction systematics $\delta W_{gs}(Z, N)$ for the fission barrier: Truran, Cameron, and Hilf [58]
IBE=1	The choice of fission barrier dependence on excitation energy $B_f(E^*)$: Barashenkov, Gereghi, Iljinov, and Toneev [27]
ISHA=2	The choice of shell correction systematics $\delta W_{gs}(Z, N)$ for the level density parameter: Truran, Cameron, and Hilf [58]
IJSP=0	The choice of fission barrier dependence on angular momentum $B_f(L)$: no dependence

TABLE VI

Optimal values for the ratio a_f/a_n in the CEM95 calculations of nucleon-induced fission cross sections for ^{208}Pb and ^{209}Bi nuclei in the 45–160 MeV region

Target nucleus	Incident particle	
	p	n
^{209}Bi	1.21	1.20
^{208}Pb	1.19	1.20

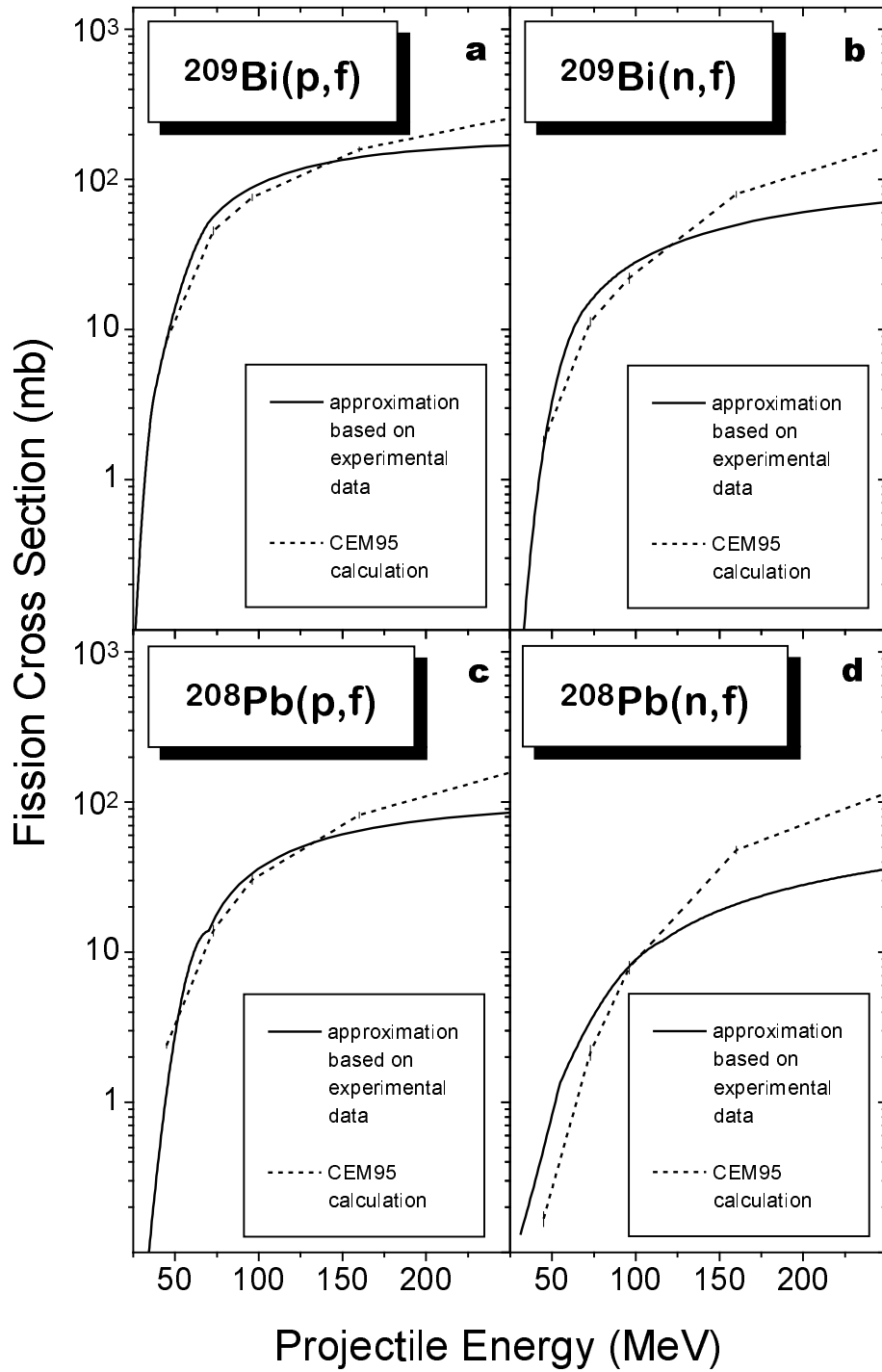


Fig. 10. Comparison between the experimental data and the calculations of the cross sections for the following reactions: $^{209}\text{Bi}(p,f)$ (a), $^{209}\text{Bi}(n,f)$ (b), $^{208}\text{Pb}(p,f)$ (c), and $^{208}\text{Pb}(n,f)$ (d). The solid lines represent the approximations of experimental data given in Sect. IV, the dashed lines show the CEM95 predictions with the input parameters shown in Tables V and VI.

VI. SENSITIVITY OF FISSION CROSS SECTIONS

Figs. 11–15 illustrate a sensitivity study of the calculated $^{209}\text{Bi}(p,f)$ cross sections relative to variations of the following CEM95 input parameters:

- the ratio of the level density parameters in the fission and neutron emission channels, a_f/a_n (Fig. 11),
- the choice of the level density parameter systematics $a(Z, N, E^*)$ (Fig. 12a, b),
- the choice of the macroscopic fission barrier model $B_f(Z, N)$ (Fig. 13a, b),
- the choice of the fission barrier dependence on excitation energy $B_f(E^*)$ (Fig. 14a),
- the choice of the fission barrier dependence on angular momentum $B_f(L)$ (Fig. 14b),
- the choice of the shell correction systematics $\delta W_{gs}(Z, N)$ for the fission barrier (Fig. 15a),
- the choice of the shell correction systematics $\delta W_{gs}(Z, N)$ for the level density parameter (Fig. 15b).

In all cases, all other parameters are held fixed as each is varied in turn. The calculational uncertainties shown in the figures are due to the statistical character of the Monte Carlo simulation.

As seen from Fig. 11, the calculated cross sections are very sensitive to even small variations of the a_f/a_n parameter. The variation of the a_f/a_n value by ± 0.03 from the optimal value of 1.21 (see Table VI), about 2.5%, makes the $^{209}\text{Bi}(p,f)$ cross section vary by a factor of 1.5–2, although the shape of the excitation function does not change appreciably.

Fig. 12 illustrates the calculations with different level density parameter systematics [56], [59]–[62]. A comparative study of these systematics and further useful references can be found in Ref. [19]. The sensitivity to the choice of the level density parameter systematics is relatively weak. The majority of these systematics give nearly the same shape to the fission excitation function (with the other parameters fixed according to Tables V and VI). The absolute scale of the excitation function varies from one model to another. For any model it is possible to improve the agreement with experiment by adjusting the a_f/a_n parameter. However, it is not possible to alter the shape of the calculated excitation function, which is typically too steep above 100 MeV. The exception is Malyshev’s systematics [59], which predicts too gently sloping an excitation function below 70 MeV. The shape closest to experiment corresponds to the choice of the 3rd Iljinov et al. systematics [56]. The same choice was found to be the optimal for the CEM in Ref. [19].

Fig. 13 illustrates the calculational results with different models of the macroscopic fission barriers [57], [63]–[68]. A comparison of results obtained with these different models for fission barriers to experimental data and further references can be found in Ref. [18]. Similarly to the previous case, the excitation function shape is too steep above 100 MeV and depends weakly on the choice of the fission-barrier model. The exception

is the choice of the constant barrier (curve 8 in Fig. 13b) that leads to a too gently sloping excitation function shape below 70 MeV. The absolute scale of the excitation function varies typically by a factor of about 2–3 depending on the choice of the specific fission barrier model, with the other parameters fixed as given in Tables V and VI. Again it is possible to improve the agreement with experiment by adjusting the a_f/a_n parameter. The best agreement with experiment was reached with the model of Krappe, Nix, and Sierk [57]. A similar conclusion was made in Ref. [18].

A similar situation takes place for the choice of the energy dependence of the fission barriers (see Fig. 14a). The systematics of Barashenkov, Gereghi, Iljinov, and Toneev [27] is found to be the optimal one (see Ref. [18] for details).

The choice of the angular momentum dependence of the fission barriers, or more exactly, the mode of calculation of the saddle-point moment of inertia according to [70] or [71] (see details in Ref. [18]) has also a rather weak influence on our present results (Fig. 14b). This is due to only a small angular momentum (of only a few \hbar) being imparted to the nucleus by incident nucleons in the energy region under study. Slightly better agreement with experiment is reached with no angular momentum dependence of the fission barriers.

Fig. 15 shows the sensitivity of our results to the choice of the shell correction systematics [58, 65, 72] for the fission barriers (Fig. 15a) and for the level density parameter (Fig. 15b). The shell corrections by Cameron [72] and Truran, Cameron, and Hilf [58] give similar results, although application of the latter option to the fission barriers (curve 2 in Fig. 15a) gives somewhat better description of the experiment above 100 MeV. This can be explained as follows. The shell corrections from Refs. [72] and [58] differ significantly only for nuclei far from stability. For these nuclei, as was pointed out in Ref. [18], the corrections [58] give a better agreement between calculated and experimentally measured fission barriers. Since the fissioning nuclei become more and more neutron-deficient with increase of incident particle energy (see Fig. 2), it is natural that Truran, Cameron, and Hilf's shell corrections [58] provide a better description of the fission cross sections at higher energies.

Results quite similar to the ones presented in Figs. 11–15 were obtained from sensitivity studies for other reactions as well. In all cases the model predicts too sharp an increase of the excitation functions for energies above 100 MeV. The higher the projectile energy, the larger are the discrepancies between the experimental data and the calculations (see Fig. 16).

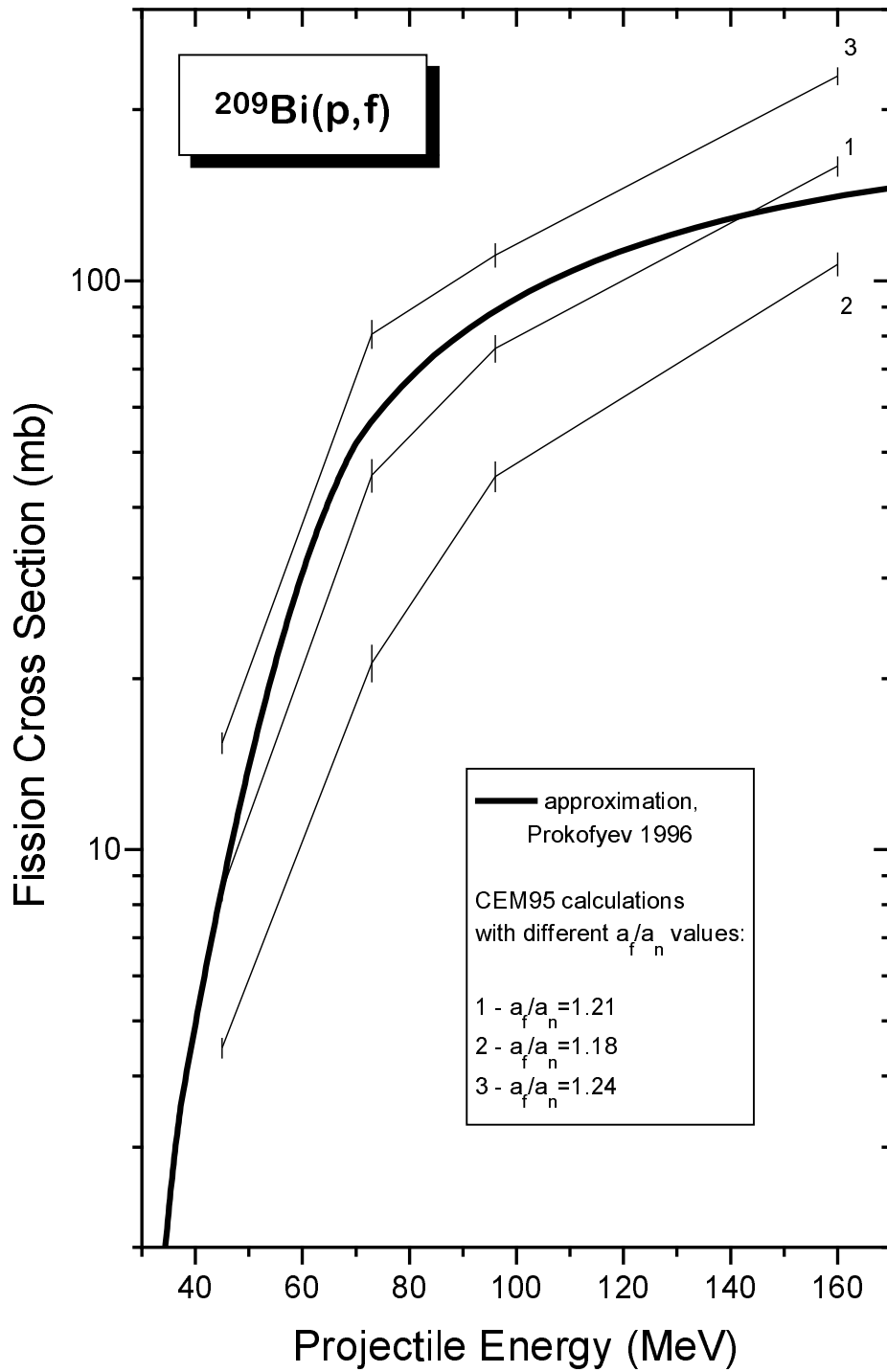


Fig. 11. The results of the sensitivity study of the $^{209}\text{Bi}(p,f)$ cross section calculation with CEM95 to the choice of the ratio of the level density parameters in the fission and neutron emission channels. The bold line is the approximation based on the experimental data. The thin lines with numbers represent the calculations with different a_f/a_n . The other model parameters are fixed according to Table V.

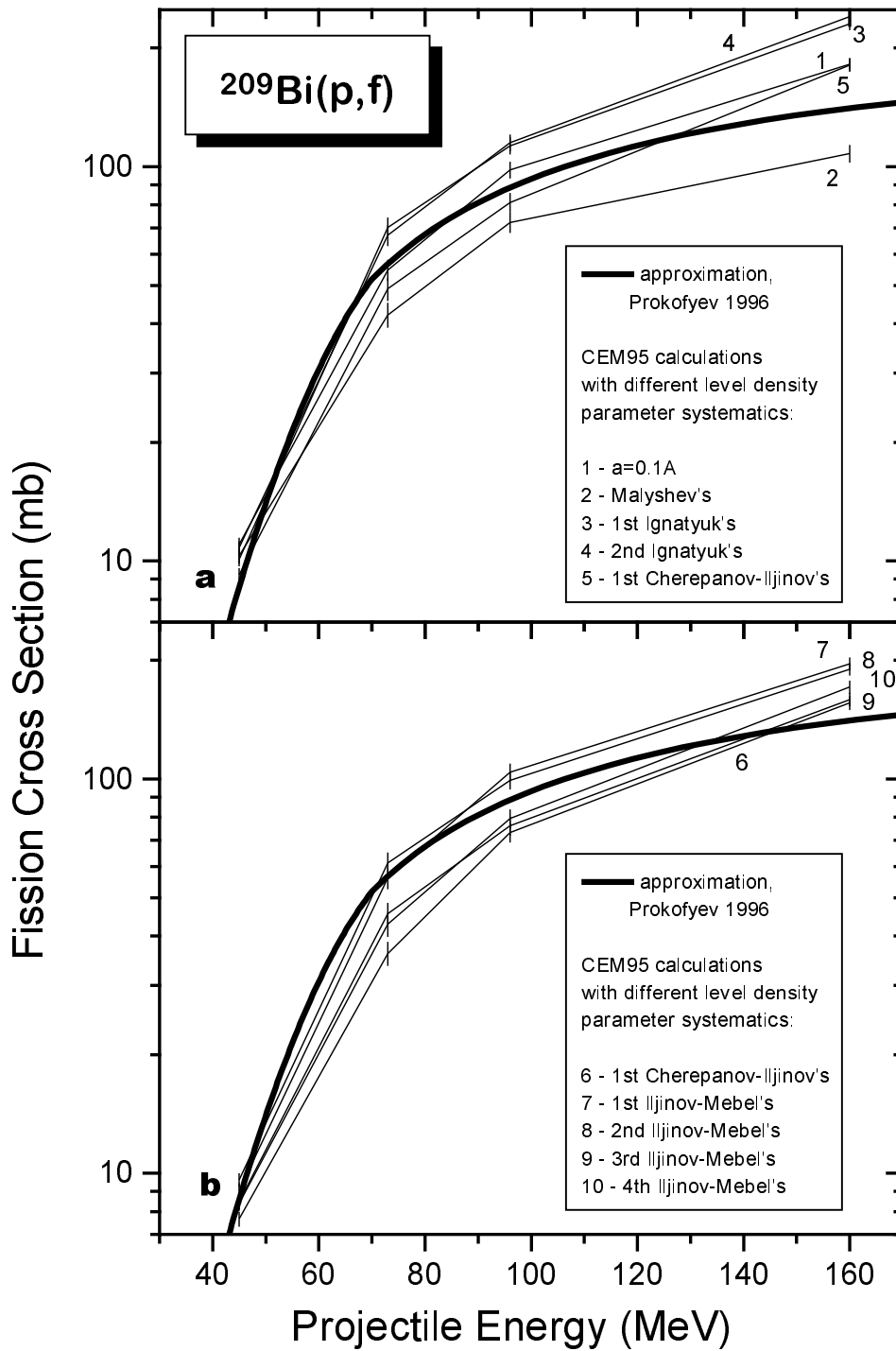


Fig. 12. The results of the sensitivity study of the $^{209}\text{Bi}(p,f)$ cross section calculation with CEM95 to the choice of the level density parameter systematics. The bold line is the approximation based on the experimental data. The thin lines with numbers represent the calculations with different level density parameter systematics [56], [59]–[62]. The other model parameters are fixed according to Tables V and VI.

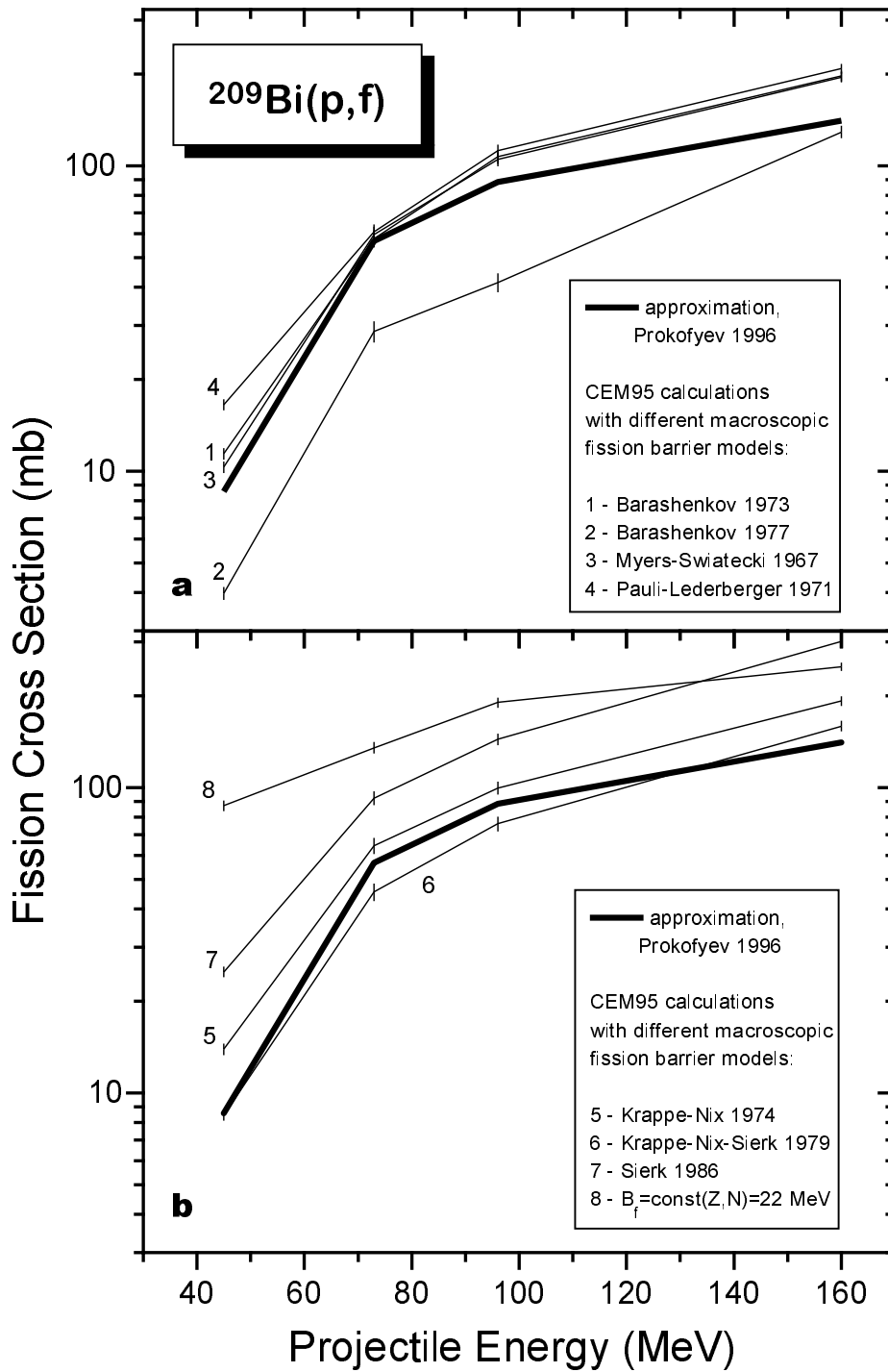


Fig. 13. The results of the sensitivity study of the $^{209}\text{Bi}(p,f)$ cross section calculation with CEM95 to the choice of the model for the macroscopic part of fission barrier. The bold line is the approximation based on the experimental data. The thin lines with numbers represent the calculations with different macroscopic fission barrier models [57], [63]–[68]. The other model parameters are fixed according to Tables V and VI.

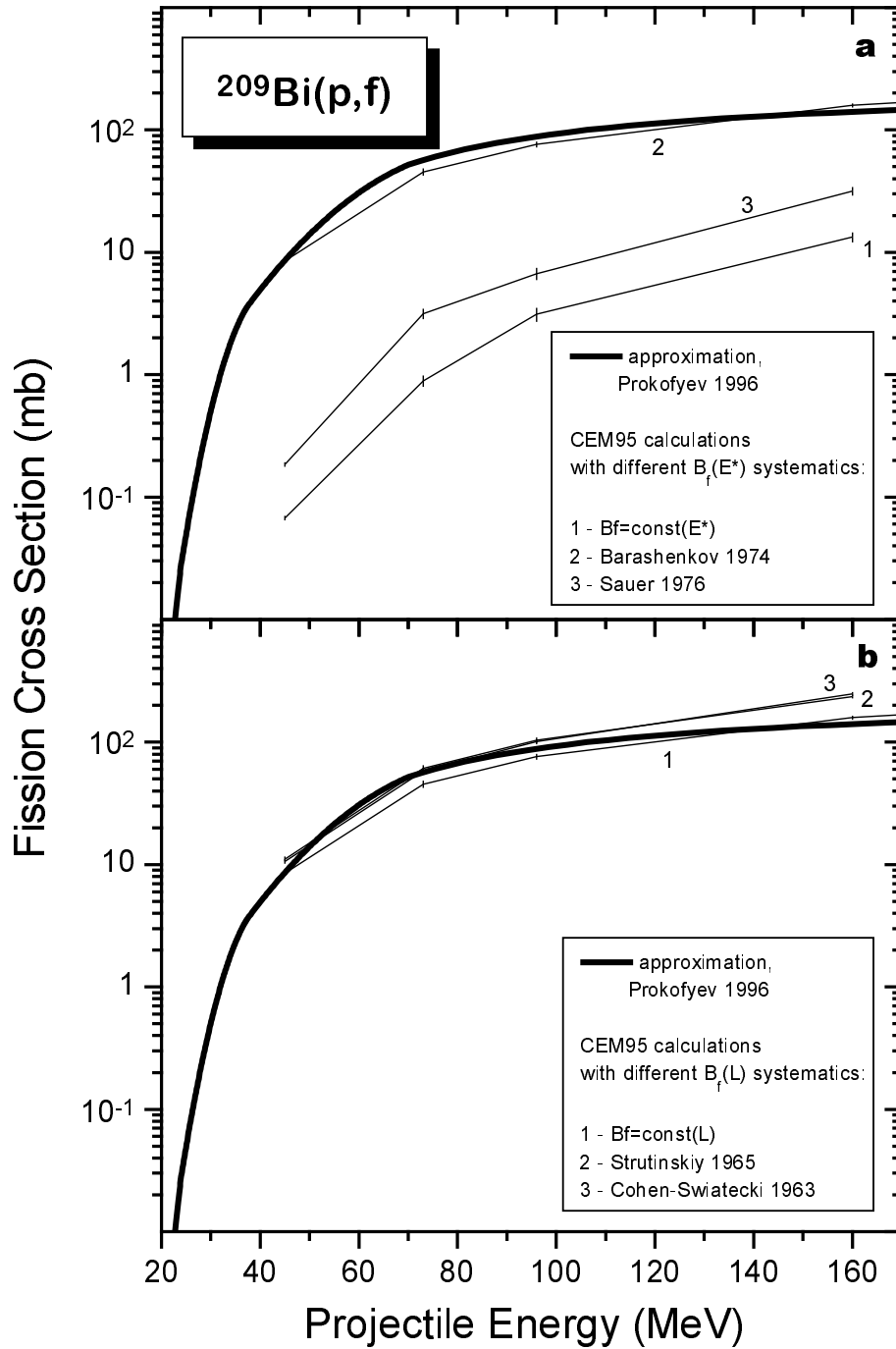


Fig. 14. The results of the sensitivity study of the $^{209}\text{Bi}(p,f)$ cross section calculation with CEM95 to the choice of the systematics for the dependence of fission barrier on excitation energy (a) and angular momentum (b). The bold line is the approximation based on the experimental data. The thin lines with numbers represent the calculations with different $B_f(E^*)$ [27, 69] and $B_f(L)$ [70, 71] systematics (see [18] for details). The other model parameters are fixed according to Tables V and VI.

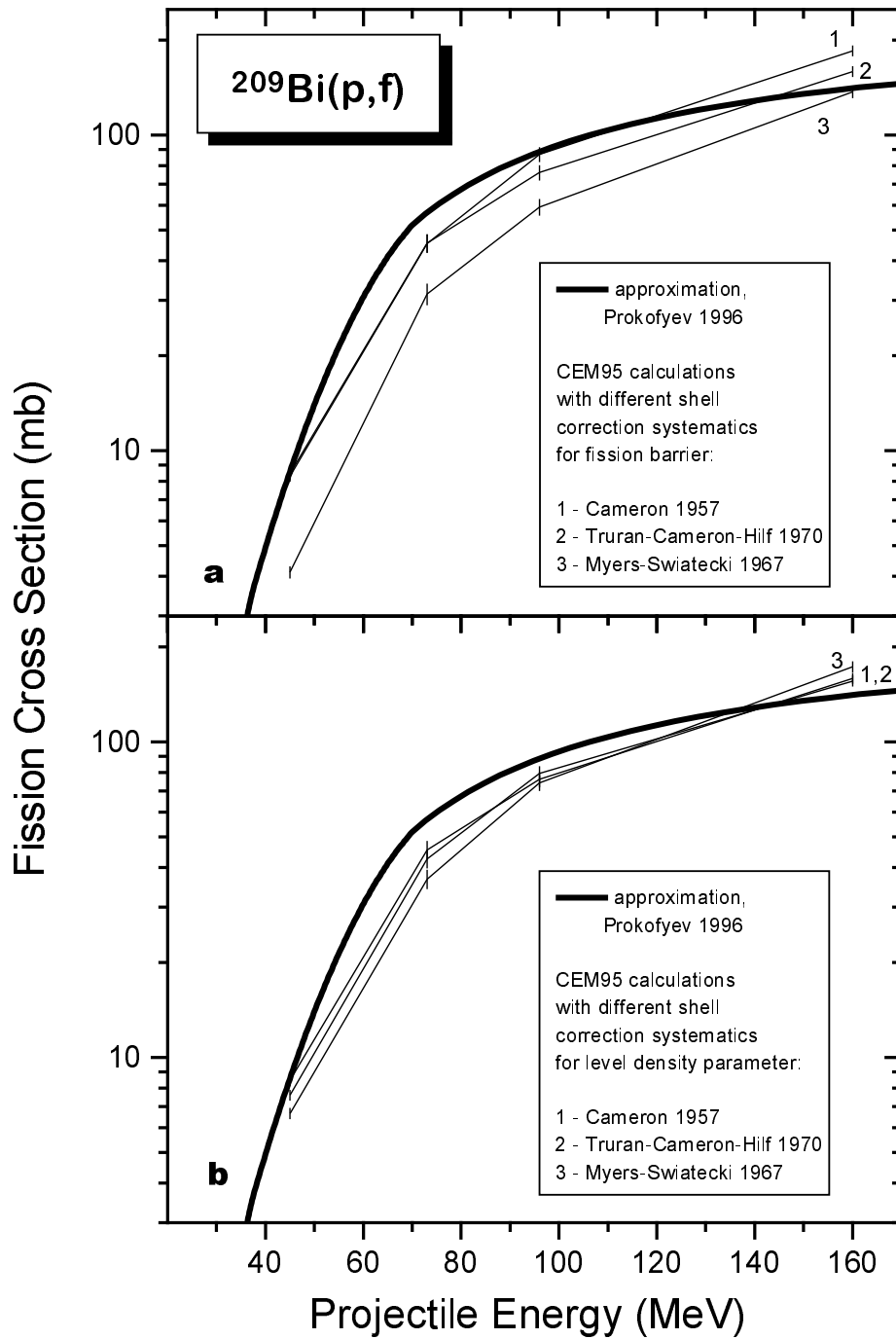


Fig. 15. The results of the sensitivity study of the $^{209}\text{Bi}(p,f)$ cross section calculation with CEM95 to the choice of the shell correction systematics for fission barrier (a) and level density parameter (b). The bold line is the approximation based on the experimental data. The thin lines with numbers represent the calculations with different shell correction systematics [58, 65, 72]. The other model parameters are fixed according to Tables V and VI.

VII. FURTHER DEVELOPMENT OF THE MODEL

Since CEM95 allows us to describe well the characteristics of nuclear reactions that do not involve fission, like double differential spectra of secondaries (see [4, 8, 9]) as well as spallation product yields (see [11]–[14]), it is natural to search for the reasons for the discrepancies in the modeling of fission. Two different possibilities are:

1) taking into account dynamical effects in fission, which reflect the connection between single-particle and collective nuclear degrees of freedom (see, for example, [73]). The diffusive character of nuclear motion towards and over the saddle point due to nuclear viscosity leads to a decrease of the value of the fission width. This effect may rise with the excitation energy, i.e., in just the direction needed for a better description of the experimental fission cross sections;

2) modification of the calculation of the level density at the saddle point. This possibility is discussed below.

As discussed previously, CEM95 incorporates several different level density parameter systematics. Most of them utilize the following formula for the excitation energy dependence of the level density parameter, which was suggested first by Ignatyuk et al. [61]:

$$a(Z, A, E^*) = \tilde{a}(A) \left[1 + \delta W(Z, A) \frac{1 - \exp[-\gamma(E^* - \Delta)]}{E^* - \Delta} \right], \quad (5)$$

where \tilde{a} is the asymptotic value of the level density parameter at high excitation energies

$$\tilde{a}(A) = \alpha A + \beta A^{2/3} B_s. \quad (6)$$

Here, A , Z , and E^* are the mass, charge, and the excitation energy of the nucleus, $\delta W(Z, A)$ is the shell correction, Δ is the pairing correction, α , β , and γ are phenomenological constants, and B_s is the surface area of the nucleus in units of the surface for the sphere of equal volume. For nuclei with equilibrium deformation $B_s \approx 1$, while for the saddle point $B_s > 1$. Formula (5) reflects the effect of the strong correlation between the single-particle state density and the shell correction magnitude for low excitation energies, and the fade out of the shell effects on the level density for high excitations [60, 61].

In the original version of CEM95, the level density parameter systematics based on formulae (5) and (6) are applied for all decay channels of an excited nucleus except for the fission channel. In the latter case, the level density parameter at the saddle point a_f is calculated using an analogous parameter for the neutron emission channel, a_n , and a constant ratio, a_f/a_n , which serves as a fitting parameter of the model. Thus the shell-effect influence on the level density in the neutron emission channel is automatically conveyed to the level density at the saddle point. On the other hand, we expect that shell corrections at the saddle point for nuclei in this mass range should bear no relation to those at the ground state, due to the large saddle-point deformation, and the consequent different microscopic level structure near the Fermi surface. In fact, the shell corrections at the saddle point should be of much smaller magnitude than those at the ground state for nuclei in the neighborhood of ^{208}Pb , due to the greatly reduced symmetry of the saddle-point shape compared to the spherical ground state (see also Refs. [74, 75]).

In order to estimate the importance of taking into account this effect, we perform calculations with the parameter a_f being *energy-independent*, which is equivalent to the disappearance of the shell-effect influence on the level density at the saddle point. The magnitude of the parameter a_f was calculated using formula (6) with the same values of the coefficients α and β that were utilized for the other decay channels. The parameter B_s was adjusted to provide the best agreement with the experimental fission cross section approximations (see Sect. IV). All the other model parameters were the same as for the calculations described in Sect. V (see Table V). The optimal values of the parameter B_s are shown in Table VII.

TABLE VII

The optimal values of the parameter B_s for the fission cross section calculations with the modified version of CEM95

Target nucleus	Incident particle	
	p	n
^{209}Bi	1.18	1.12
^{208}Pb	1.15	1.12

The values for the parameter B_s are physically reasonable because they are larger than 1, which reflects the larger deformation of the fissioning nucleus at the saddle point in comparison with the equilibrium state and they are not far from the value $B_s \approx 2^{1/3}$, which is expected for the saddle-point configuration of the preactinides [76]. However, we do not yet understand why different values are needed for proton- and neutron-induced fission, and why the values of B_s in the neutron channel are significantly smaller than those corresponding to the known deformation of saddle-point shapes in this mass region.

The ratio a_f/\tilde{a}_n , where \tilde{a}_n is the asymptotic (large E^*) level density parameter in the neutron channel, is fixed by the fitting of B_s , and is not independently fitted as was done previously. \tilde{a}_n is calculated using formula (6) and the values $\alpha = 0.072$ and $\beta = 0.257$, which correspond to the 3rd Iljinov et al. systematics [56]. The ratios appear to depend only weakly on the nuclear mass. For the reactions under study their values (given in Fig. 16) are in the range 1.045–1.070, which are consistent with the compilation of \tilde{a}_f/\tilde{a}_n values published by Ignatyuk et. al. [76].

The results of calculations with the modified CEM95 are shown in Fig. 16. We see a much better description of the experimental fission cross sections in comparison with the original version for nucleon energies of 100–500 MeV. On the other hand, the calculation systematically overestimates to a slight extent the fission cross sections below 100 MeV. We emphasize that other related improvements need to be made before a final assessment of the model's value and predictive capability can be made. For example, an expected excitation- energy dependence of the ground-state shell correction would change the average height of the calculated fission barriers as the incident energy is increased. However, the current modifications do indicate the crucial importance of properly incorporating appropriate level densities and motivate the search for a consistent model of barriers, ground-state masses, and level densities which may improve the predictive power of the CEM.

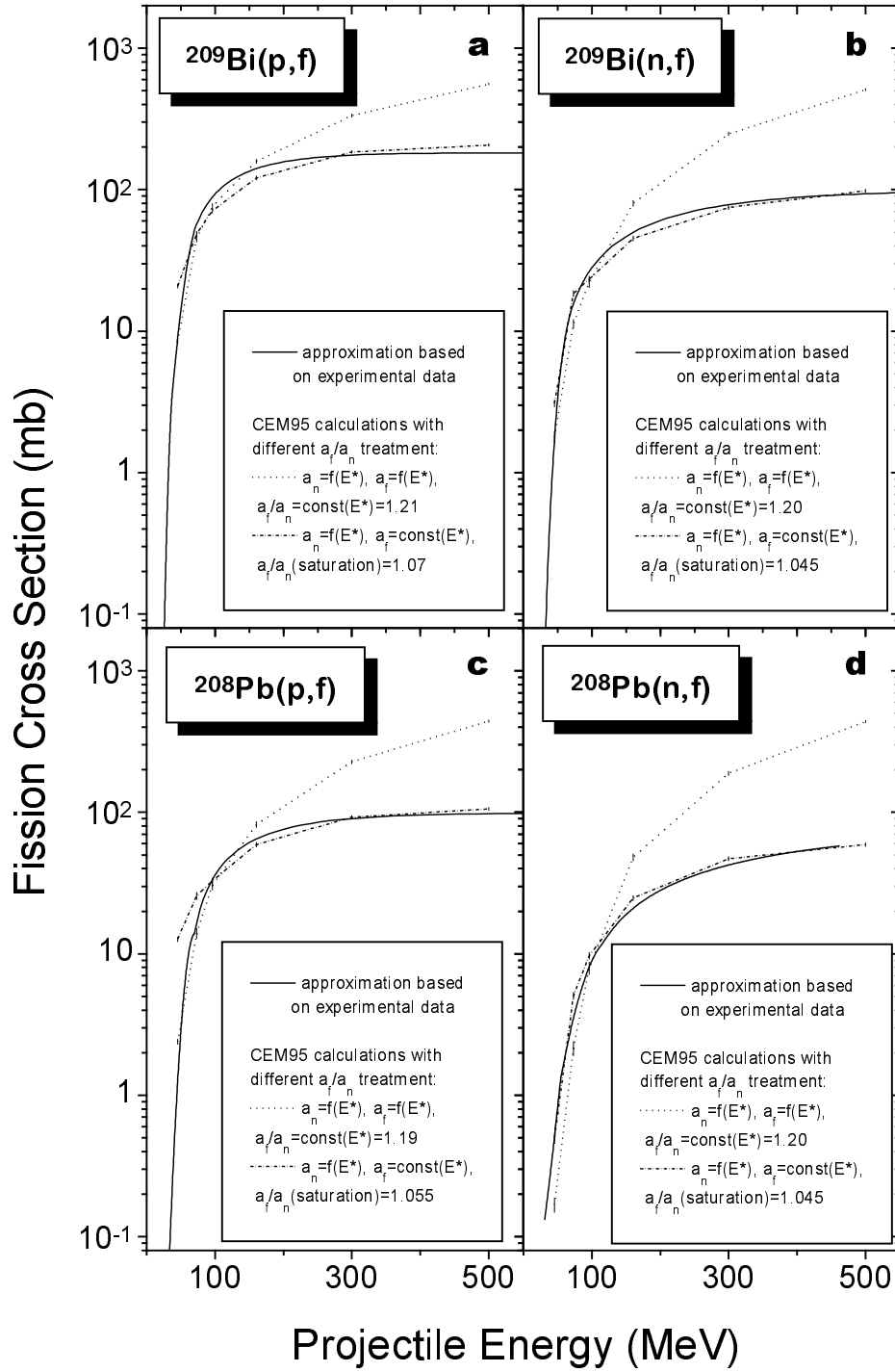


Fig. 16. Comparison of the experimental data on the $^{209}\text{Bi}(p,f)$ (a), $^{209}\text{Bi}(n,f)$ (b), $^{208}\text{Pb}(p,f)$ (c), and $^{208}\text{Pb}(n,f)$ (d) cross sections and the calculations with the original and modified versions of CEM95. The solid lines represent the approximation of the experimental data (see Sec. IV). The dotted lines show the original CEM95 results with the parameters given in Tables V and VI. The dot-dashed lines show the results after the modification of the fission channel in CEM95.

VIII. SUMMARY

We have performed a systematic analysis of the nucleon-induced fission cross sections for ^{209}Bi and ^{208}Pb nuclei in the 45–500 MeV energy range using the CEM95 code, which has incorporated several choices for the level density parameters, nuclear masses, shell and pairing corrections, saddle-point moments of inertia, and for the macroscopic and microscopic fission barriers. We have performed a detailed analysis of the dependence of calculated fission cross sections and of distributions of the residual nuclei after the cascade stage of reactions and of fissioning nuclei at the compound-nucleus stage of reactions on all these choices. We find that the distributions of residual and fissioning nuclei with respect to their mass, charge, and excitation energy are not very sensitive to the specific model choices used in our calculations. Also, our results agree satisfactorily with the scanty data available in the literature for the average share of the linear momentum transferred to the fissioning nuclei.

We present here analytical approximations determined by a critical analysis of all available experimental data, and compare them to calculations using CEM95 with and without modifications. Our analysis shows that by choosing the appropriate value for the ratio of the level density parameters in the fission and neutron emission channels a_f/a_n , it is possible to describe satisfactorily fission cross sections of all reactions under investigation in a limited range of energy. But it is impossible to get a satisfactory agreement in the whole range of energy using a fixed set of CEM95 parameters and of nuclear models used in the calculations. This means that the version of the CEM as realized in the code CEM95 does not allow us to predict arbitrary fission cross sections in a large range of incident energies. We perform in the present work a further development of the model, where we have modified the calculation of the level density parameter of nuclei at the saddle point, by use of simple physical considerations. This change allows us to get much better agreement with the experimental fission cross sections in the energy region from 100 to 500 MeV, but further improvement of the CEM95 is still needed at energies below about 100 MeV. We plan to continue our work by extending the range of incident energies and of nuclear targets investigated, striving for a model capable of predicting fission cross sections for arbitrary targets in a wide range of incident energies.

ACKNOWLEDGMENTS

It is a pleasure to acknowledge E. A. Cherepanov, V. P. Eismont, M. G. Itkis, V. A. Konshin, D. G. Madland, P. Möller, J. R. Nix, and R. J. Peterson for useful discussions on fission physics.

This study was partially supported by the U. S. Department of Energy.

REFERENCES

- [1] “*Proc. Second Int. Conf. on Accelerator-Driven Transmutation Technologies and Applications*,” Kalmar, Sweden, June 3–7, 1996, Vols. 1 and 2, H. CONDÉ, Ed., Uppsala University (1997).

- [2] “*Proc. Int. Workshop on Nucl. Methods for Transmutation of Nuclear Wastes: Problems, Perspectives, Cooperative Research*,” Dubna, Russia, May 29–31, 1996, M. Kh. KHANKHASAYEV, Zh. B. KURMANOV, and H. PLENDL, Eds., World Scientific, Singapore (1997).
- [3] K. K. GUDIMA, S. G. MASHNIK, and V. D. TONEEV, “Cascade-Exciton Model of Nuclear Reactions,” *Nucl. Phys.* **A401**, 329 (1983).
- [4] S. G. MASHNIK, “The Cascade-Exciton Approach for Intermediate Energy Nuclear Reactions,” *Proc. 7th Int. Conf. on Nuclear Reaction Mechanisms*, Varenna, June 6–11, 1994, E. GADIOLI, Ed., Università degli Studi di Milano (1994), p. 100.
- [5] S. G. MASHNIK, “Neutron-Induced Particle Production in the Cumulative and Non-cumulative Regions at Intermediate Energies,” *Nucl. Phys.* **A568**, 703 (1994).
- [6] S. G. MASHNIK, “How Many Nucleons Are Required for Nuclear Pion Absorption?” *Yad. Fiz.* **58**, 1772 (1995) [*Phys. At. Nucl.* **58**, 1672 (1995)]; see also “Low- and Intermediate-Energy Pion-Nucleus Interactions in the Cascade-Exciton Model,” *Acta Phys. Pol. B* **24**, 1685 (1993); see also “Stopped Pion Absorption by Nuclei in the Cascade-Exciton Model,” *Rev. Roum. Phys.* **37**, 179 (1992).
- [7] T. GABRIEL, G. MAINO, and S. G. MASHNIK, “Analysis of Intermediate Energy Photonuclear Reactions,” Proc. XII Int. Sem. on High Energy Probl. *Relativistic Nucl. Phys. & Quantum Chromodynamics*, Dubna, Russia, 12–17 September, 1994, A. M. BALDIN and V. V. BUROV, Eds., JINR E1, 2-97-79 (1997) p. 309.
- [8] M. BLANN, H. GRUPPELAR, P. NAGEL, and J. RODENS, *International Code Comparison for Intermediate Energy Nuclear Data*, NEA OECD, Paris (1994).
- [9] S. G. MASHNIK, “Physics of the CEM92M Code,” *Proc. Specialists’ Mtg. “Intermediate Energy Nuclear Data: Models and Codes*,” Issy-les-Moulineaux, France, May 30–June 1, 1994, OECD, Paris (1994). p. 107.
- [10] S. G. MASHNIK, “Analysis of Excitation Functions of Proton-Nucleus Reactions within the Cascade-Exciton Model,” *Izv. Rossiiskoi Akad. Nauk, ser. fiz.* **60**, 73 (1996) [*Bull. Russian Acad. Sci.: Physics* **60**, 58 (1996)].
- [11] S. G. MASHNIK, A. J. SIERK, O. BERSILLON, and T. A. GABRIEL, “Cascade-Exciton Model Detailed Analysis of Proton Spallation at Energies From 10 MeV to 5 GeV,” Los Alamos National Laboratory Report LA-UR-97-2905 (1997); <http://t2.lanl.gov/publications/publications.html>.
- [12] Yu. E. TITARENKO, O. V. SHVEDOV, M. M. IGUMNOV, R. MICHEL, S. G. MASHNIK, E. I. KARPIKHIN, V. D. KAZARITSKY, V. F. BATYAEV, A. B. KOLDOBSKY, V. M. ZHIVUN, A. N. SOSNIN, R. E. PRAEL, M. B. CHADWICK, T. A. GABRIEL, and M. BLANN, “Experimental and Theoretical Study of the Yields of Radionuclides Produced in ^{209}Bi Thin Targets Irradiated by 130 MeV and 1.5 GeV Protons,” Los Alamos National Laboratory Report LA-UR-97-3787 (1997); E-print *nucl-th/9709056*; to be published in *Nucl. Instr. Meth. A*.

- [13] K. A. VAN RIPER, S. G. MASHNIK, M. B. CHADWICK, M. HERMAN, A. J. KONING, E. J. PITCHER, A. J. SIERK, G. J. VAN TUYLE, L. S. WATERS, and W. B. WILSON, “APT Medical Isotope Production Study: ^{18}F and ^{131}I Production,” Los Alamos National Laboratory Report LA-UR-97-5068 (1997); <http://t2.lanl.gov/publications/publications.html>.
- [14] R. MICHEL and P. NAGEL, *International Codes and Model Intercomparison for Intermediate Energy Activation Yields*, NSC/DOC(97)-1, NEA/P/&T No 14, OECD, Paris (1997); <http://www.nea.fr/html/science/pt/ieay>.
- [15] V. A. KONSHIN, “Calculation of Neutron and Proton Induced Reaction Cross Sections for Actinides in the Energy Region from 10 MeV to 1 GeV,” *JAERI-Research 95-036*, JAERI (1995).
- [16] V. S. BARASHENKOV and V. D. TONEEV, *Interaction of High Energy Particles and Nuclei with Atomic Nuclei*, (in Russian) Atomizdat, Moscow (1972).
- [17] K. K. GUDIMA, G. A. OSOSKOV, and V. D. TONEEV, “Model for Pre-Equilibrium Decay of Excited Nuclei,” *Yad. Fiz.* **21**, 260 (1975) [*Sov. J. Nucl. Phys.* **21**, 138 (1975)];
S. G. MASHNIK and V. D. TONEEV, “MODEX — the Program for Calculation of the Energy Spectra of Particles Emitted in the Reactions of Pre-Equilibrium and Equilibrium Statistical Decays,” *JINR Communication P4-8417*, Dubna (1974).
- [18] S. G. MASHNIK, “Optimal Systematics of Single-Humped Fission Barriers for Statistical Calculations,” *Acta Phys. Slovaca* **43**, 243 (1993).
- [19] S. G. MASHNIK, “Statistical Model Calculations of Nuclear Level Density with Different Systematics for the Level Density Parameter,” *Acta Phys. Slovaca* **43**, 86 (1993).
- [20] S. G. MASHNIK, “User Manual for the Code CEM95,” OECD Nuclear Energy Agency Data Bank, Le Saint-Germain 12, Boulevard des Iles, F-92130, Issy-les-Moulineaux, Paris, France (1995); <http://www.nea.fr/abs/html/iaea1247.html>.
- [21] P. STAPLES, private communication.
- [22] V. P. EISMONT, A. V. PROKOFIEV, A. N. SMIRNOV, K. ELMGREN, J. BLOMGREN, H. CONDÉ, J. NILSSON, N. OLSSON, T. RÖNNQVIST, E. TRANÉUS, “Relative and Absolute Neutron-Induced Fission Cross Section of ^{208}Pb , ^{209}Bi , and ^{238}U in the Intermediate Energy Region,” *Phys. Rev. C* **53**, 2911 (1996).
- [23] V. P. EISMONT, A. V. PROKOFIEV, A. N. SMIRNOV, K. ELMGREN, J. BLOMGREN, H. CONDÉ, J. NILSSON, N. OLSSON, E. RAMSTRÖM, “Measurements of Neutron-Induced Fission Cross Sections of Heavy Nuclei in the Intermediate Energy Region,” pp. 606–612 in [1].

- [24] V. P. EISMONT, A. V. KIREEV, I. V. RYZHOV, I. V. TUTIN, H. CONDÉ, K. ELMGREN, S. HULTQVIST, “Measurements of Neutron-Induced Fission Cross Sections of ^{209}Bi at 45 and 73 MeV,” pp. 618–623 in [1].
- [25] H. CONDÉ, “Cross Section Standards Above 20 MeV,” *Proc. Int. Conf. on Nuclear Data for Science and Technology*, Gatlinburg, Tennessee, May 9–13, 1994, J. K. DICKENS, Ed., American Nuclear Society (1994) Vol. 1, p. 53.
- [26] A. D. CARLSON, S. CHIBA, F.-J. HAMBSCH, N. OLSSON, and A. N. SMIRNOV, “Update to Nuclear Data Standards for Nuclear Measurements,” IAEA Report INDC (NDS)-368, Vienna (1997); *Proc. Int. Conf. on Nuclear Data for Science and Technology*, Trieste, Italy, May 19–24, 1997 (to be published).
- [27] V. S. BARASHENKOV, F. G. GEREGHI, A. S. ILJINOV, and V. D. TONEEV, “Inelastic Interactions of High Energy Nucleons with Heavy Nuclei,” *Nucl. Phys.* **A222**, 204 (1974).
- [28] I. Yu. GORSHKOV, A. T. DIACHENKO, A. V. PROKOFIEV, A. N. SMIRNOV, and V. P. EISMONT, “Momentum Transfer in Reactions of Medium-Energy Protons with Heavy Nuclei,” *Izv. Akad. Nauk, Ser. Fiz.* **57**, 178 (1993) [*Bull. Russian Acad. Sci.: Physics* **57**, 1274 (1993)].
- [29] L. KOWALSKI and C. STEPHAN, “Distributions Angulaires et Sections Efficaces de la Fission de l’Uranium, le Bismuth a l’Or Induite par des Protons de 156 MeV,” *J. de Physique* **24**, 901 (1963).
- [30] C. STEPHAN, F. MAURY, J. PETER, and H. LANGEVIN-JOLIOT, “Fission de l’Uranium et du Bismuth induite par des Protons de 96 MeV,” *Annuaire 1965*, Institut de Physique Nucléaire, Faculés des Sciences de Paris et d’Orsay (1965) p. 13.
- [31] O. E. SHGAEV, V. S. BYCHENKOV, M. F. LOMANOV, A. I. OBUKHOV, N. A. PERFILOV, G. G. SHIMCHUK, and R. M. YAKOVLEV, “Observation of the Effect of Central Collision Leading to Formation of a Compound Nucleus in Interaction of 200 MeV Protons with Nuclei,” *Yad. Fiz.* **27**, 1424 (1978) [*Sov. J. Nucl. Phys.* **27**, 751 (1978)]; O. E. SHGAEV, Ph. D. Thesis, Khlopin Radium Institute, Leningrad (1974); O. E. SHGAEV, private communication.
- [32] V. P. EISMONT, A. V. KIREEV, I. V. RYZHOV, G. A. TUTIN, J. BLOMGREN, H. CONDÉ, K. ELMGREN, N. OLSSON, J. RAHM, E. RAMSTRÖM, “Neutron-Induced Angular and Kinetic Energy Distributions for ^{209}Bi and ^{238}U at 75 MeV,” *Proc. Int. Conf. on Nuclear Data for Science and Technology*, Trieste, Italy, May 19–24, 1997 (to be published).
- [33] I. HALPERN, “Nuclear Fission,” *Ann. Rev. Nucl. Sci.* **9**, 245 (1959); *Nuclear Fission*, (in Russian) Fizmatgiz, Moscow (1962).
- [34] Yu. P. GANGRSKY, B. DALKHSUREN, B. N. MARKOV, *Nuclear Fission Fragments*, Handbook (in Russian) Atomizdat, Moscow, (1986).

- [35] V. P. EISMONT, A. I. OBUKHOV, A. V. PROKOFIEV, and A. N. SMIRNOV, “An Experimental Database on Proton-Induced Fission Cross Sections of Tantalum, Tungsten, Lead, Bismuth, Thorium and Uranium,” pp. 592–598 in [1].
- [36] O. E. SHIGAEV, V. S. BYCHEKOV, M. F. LOMANOV, A. I. OBUKHOV, N. A. PERFILOV, G. G. SHIMCHUK, and R. M. YAKOVLEV, “Determination of the Anisotropy and Fission Cross Sections of Nuclei Bombarded by 200 MeV Protons as Functions of Z^2/A ,” (in Russian) Khlopin Radium Institute Preprint No. 17 (1973); B. A. BOCHAGOV, V. S. BYCHENKOV, V. D. DMITRIEV, S. P. MALTSEV, A. I. OBUKHOV, N. A. PERFILOV, V. A. UDOD, and O. E. SHIGAEV, “Determination of the Fission Cross Section of ^{232}Th , ^{209}Bi , $^{208-206}\text{Pb}$, ^{197}Au , ^{181}Ta , Yb, and Sm Bombarded by 1 GeV Protons,” *Yad. Fiz.* **28**, 572 (1978) [*Sov. J. Nucl. Phys.* **28**, 291 (1978)].
- [37] V. N. OKOLOVICH, O. A. ZHUKOVA, M. G. ITKIS, S. I. MULGIN, “Fission of Some Pre-Actinide Nuclei in the (p,f) Reaction,” (in Russian) Institute of Nuclear Physics, Academy of Science of the Kazakh S.S.R. Preprint P-112, Alma-Ata (1974); O. A. ZHUKOVA, A. V. IGNATYUK, M. G. ITKIS, S. I. MULGIN, V. N. OKOLOVICH, G. N. SMIRENKIN, and A. S. TISHIN, “Fission of Pre-Actinide Nuclei. The (p,f) Reaction in the Proton Energy Region 24–30 MeV,” *Yad. Fiz.* **26**, 473 (1977) [*Sov. J. Nucl. Phys.* **26**, 251 (1977)].
- [38] A. V. IGNATYUK, M. G. ITKIS, I. A. KAMENEV, S. I. MULGIN, V. N. OKOLOVICH, and G. N. SMIRENKIN, “Study of the Fissility of Preactinide Nuclei by Protons and α Particles,” *Yad. Fiz.* **40**, 625 (1984) [*Sov. J. Nucl. Phys.* **40**, 400 (1984)].
- [39] A. KHODAI-JOOPARI, Ph.D. Thesis, Report UCRL-16489, Berkeley (1966).
- [40] E. GADIOLI, I. IORI, N. MOLHO, and L. ZETTA, “Fission Fragment Angular Distribution in Proton-Induced Fission of ^{209}Bi ,” *Lett. Nuovo Cimento* **2**, 904 (1969).
- [41] W. F. BILLER, Ph.D. Thesis, Report UCRL-2067, Berkeley (1953).
- [42] L. G. JODRA and N. SUGARMAN, “High-Energy Fission of Bismuth. Proton Energy Dependence,” *Phys. Rev.* **99**, 1470 (1955).
- [43] P. KRUGER and N. SUGARMAN, “High-Energy Fission of Bismuth. Nuclear Charge Dependence,” *Phys. Rev.* **99**, 1459 (1955).
- [44] V. P. SHAMOV, “Mechanisms of Heavy Nuclei Fission at High Excitation Energies,” (in Russian) *Doklady Akademii Nauk SSSR* **103**, 593 (1955).
- [45] H. M. STEINER and J. A. JUNGERMAN, “Proton-Induced Fission Cross Sections for U^{238} , U^{235} , Th^{232} , Bi^{209} , and Au^{197} at 100 to 340 MeV,” *Phys. Rev.* **101**, 807 (1956).
- [46] A. K. LAVRUKHINA and L. D. KRASAVINA, “Fission of Heavy Nuclei Elements by High Energy Particles,” (in Russian) *Atomnaya Energya* **2**, 27 (1957).

- [47] T. T. SUGIHARA, J. ROESMER, and J. W. MEADOWS, “Asymmetric Fission of Bismuth,” *Phys. Rev.* **121**, 1179 (1961).
- [48] V. A. KONSHIN, E. S. MATUSEVICH, and V. I. REGUSHEVSKIĬ, “Cross Sections for Fission of Ta¹⁸¹, Re, Pt, Au¹⁹⁷, Pb, Bi²⁰⁹, Th²³², U²³⁵, and U²³⁸ by 150–660 MeV Protons,” *Yad. Fiz.* **2**, 682 (1965) [*Sov. J. Nucl. Phys.* **2**, 489 (1966)].
- [49] M. MAURETTE and C. STEPHAN, “Mesures de Sections Efficaces Absolues de Fission Induite par des Protons de 156 MeV, Utilisant le Mica Comme Detecteur de Fragments de Fission,” *Proc. Int. Symp. on Physics and Chemistry of Fission*, Vienna, 1965, Vol. 2, p. 307 (1967).
- [50] G. N. FLEROV, V. P. PERELYGIN, and O. OTGONSUREN, “On the Origin of Fission Fragment Tracks in Lead Glasses,” (in Russian) *Atomnaya Energiya* **33**, 979 (1972).
- [51] A. A. REUT, G. I. SELIVANOV, and V. V. YURIEV, *Institute of Nuclear Problems of the U.S.S.R. Academy of Science Report*, Moscow (1950).
- [52] P. E. VOROTNIKOV and L. S. LARIONOV, “Cross Sections for Neutron Fission of Pb and Bi,” *Yad. Fiz.* **40**, 867 (1984) [*Sov. J. Nuc. Phys.* **40**, 552 (1984)].
- [53] V. I. GOLDANSKY, V. S. PENKINA, and E. Z. TARUMOV, “Fission of Heavy Nuclei by High Energy Neutrons,” (in Russian) *Zh. Eksp. Teor. Fiz.* **29**, 778 (1955).
- [54] T. FUKAHORI and S. PEARLSTEIN, “Evaluation at the Medium Energy Region for Pb-208 and Bi-209,” *Proc. of the Advisory Group Meeting on Intermediate Energy Nuclear Data for Applications Organized by IAEA*, Vienna, October 9–12, 1990, Report INDC(NDS)-245, Vienna (1991), p. 93.
- [55] I. DOSTROVSKY, Z. FRAENKEL, and G. FRIEDLANDER, “Monte Carlo Calculations of Nuclear Evaporation Processes. III. Application to Low-Energy Reactions,” *Phys. Rev.* **116**, 683 (1959).
- [56] A. S. ILJINOV, M. V. MEBEL, N. BIANCHI, E. De SANCTIS, C. GUARDALO, V. LUCHERIINI, V. MUCCIFORA, E. POLLI, A. R. REOLON, and P. ROSSI, “Phenomenological Statistical Analysis of Level Densities, Decay Width and Lifetimes of Excited Nuclei,” *Nucl. Phys.* **A543**, 517 (1992).
- [57] H. J. KRAPPE, J. R. NIX, and A. J. SIERK, “Unified Nuclear Potential for Heavy-Ion Elastic Scattering, Fusion, Fission, and Ground-State Masses and Deformations,” *Phys. Rev. C* **20**, 992 (1979).
- [58] J. W. TRURAN, A. G. W. CAMERON, and E. HILF, “Construction of Mass Formulas Designed to be Valid for Neutron-Rich Nuclei,” *Proc. Int. Conf. on the Properties of Nuclei Far From the Region of Beta-Stability*, Leysin, Switzerland, 1970, Vol. 1, p. 275.
- [59] A. V. MALYSHEV, *Level Density and Structure of Atomic Nuclei*, (in Russian) Atomizdat, Moscow (1969).

- [60] A. V. IGNATYUK, G. N. SMIRENKIN, and A. S. TISHIN, “Phenomenological Description of the Energy Dependence of the Level Density Parameter,” *Yad. Fiz.* **21**, 485 (1975) [*Sov. J. Nucl. Phys.* **21**, 255 (1975)].
- [61] A. V. IGNATYUK, M. G. ITKIS, V. N. OKOLOVICH, G. N. SMIRENKIN, and A. S. TISHIN, “Fission of Pre-Actinide Nuclei. Excitation Functions for the (α, f) Reactions,” *Yad. Fiz.* **21**, 1185 (1975) [*Sov. J. Nucl. Phys.* **21**, 612 (1975)].
- [62] E. A. CHEREPANOV and A. S. ILJINOV, “Statistical Calculation of Nuclear Level Densities,” (in Russian) *Nucleonika* **25**, 611 (1980).
- [63] V. S. BARASHENKOV, A. S. ILJINOV, V. D. TONEEV, and F. G. GEREGHI, “Fission and Decay of Excited Nuclei,” *Nucl. Phys.* **A206**, 131 (1973).
- [64] V. S. BARASHENKOV and F. G. GEREGHI, “Systematics of Fission Barriers,” (in Russian) *Communication JINR, P4-10781*, Dubna (1977).
- [65] W. D. MYERS and W. J. SWIATECKI, “Anomalies in Nuclear Masses,” *Ark. Fysik* **36**, 343 (1967).
- [66] H. C. PAULI and T. LEDERGERBER, “Fission Threshold Energies in the Actinide Region,” *Nucl. Phys.* **A175**, 545 (1971).
- [67] H. J. KRAPPE and J. R. NIX, “Modified Definition of the Surface Energy in the Liquid Drop Formula,” *Proc. 3rd IAEA Symp. on the Phys. and Chemistry of Fission*, Rochester, New York, 1973 (IAEA-SM-174/12, Vienna, 1974), v. 1, p. 159.
- [68] A. J. SIERK, “Macroscopic Model of Rotating Nuclei,” *Phys. Rev. C* **33**, 2039 (1986).
- [69] G. SAUER, H. CHANDRA, and U. MOSEL, “Thermal Properties of Nuclei,” *Nucl. Phys.* **A264**, 221 (1976).
- [70] V. M. STRUTINSKIĬ, “Form of the Fissioning Nucleus at the Saddle Point and the Liquid-Drop Model,” *Yad. Fiz.* **1**, 821, (1965) [*Sov. J. Nucl. Phys.* **1**, 588, (1965)].
- [71] S. COHEN and W. J. SWIATECKI, “The Deformation Energy of a Charged Drop. Part V: Results of Electronic Computer Studies,” *Ann. Phys. (N.Y.)* **22**, 406 (1963).
- [72] A. G. W. CAMERON, “A Revised Semiempirical Atomic Mass Formula,” *Can. J. Phys.* **35**, 1021 (1957).
- [73] H. A. WEIDENMÜLLER, “Dissipation Mechanisms,” *Nucl. Phys.* **A502**, 387c (1989).
- [74] A. S. ILJINOV, E. A. CHEREPANOV, and S. E. CHIGRINOV, “Probability of Fission by Particles of Intermediate Energy,” *Yad. Fiz.* **32**, 322 (1980) [*Sov. J. Nucl. Phys.* **32**, 166 (1980)].
- [75] G. GIARDINA, “Sensitivity of the Evaporation Residue Cross Sections of Highly Fissile and Neutron Deficient Nuclei,” (in English) *Yad. Fiz.* **57**, 1277 (1994).

- [76] A. V. IGNATYUK, G. N. SMIRENKIN, M. G. ITKIS, S. I. MULGIN, and V. N. OKOLOVICH, "Fissility of Preactinides in Charged-Particle Induced Reactions," *Fiz. Elem. Chastits At. Yadra* **16**, 709 (1985) [*Sov. J. Part. Nucl.* **16**, 307 (1985)].